Solid Core Holey Photonic Crystal Fiber for High Optical Confinement & Tailored Dispersion

Dissertation Submitted in the partial fulfilment of requirement for the award of degree of

Master of Engineering

In

Electronics and Communication Engineering

Submitted by:

Vikas Garg

(801261029)

Under the guidance of:

Dr. Mukesh Kumar

ELECTRONICS AND COMMUNICATION ENGINEERING DEPARTMENT

THAPAR UNIVERSITY

(Established under the section 3 of UGC Act, 1956)

PATIALA – 147004 (PUNJAB) July 2014

DECLARATION

I Vikas Garg, hereby declare that the work which is being presented in this dissertation entitled "Solid Core Holey Photonic Crystal Fiber for High optical Confinement & Tailored Dispersion" by me in partial fulfilment of the requirement for the award of degree of Master of Engineering in Electronics and Communication Engineering from Thapar University, Patiala, is an authentic record of my own work carried out under the supervision of **Dr. Mukesh Kumar**

The matter presented in this dissertation has not been submitted in any other university/institute for the award of any other degree.

Date: 14/07/2014

Vikas Garg

(801261029)

It is certified that the above statement made by the student is correct to the best of my knowledge and belief.

Date: 14/07/2014

Dr. Mukesh Kumar

Assistant Professor

ECED

Countersigned by:-

Dr. Sanjay Sharma

Professor and Head ECED

Thapar University Patial

Dr. S.K.Mohapatra

Dean of Academic Affairs

Thapar University, Patiala

TABLE OF CONTENTS

ACKNOWLEDGEMENT

I would like to express my special thanks and deep sense of gratitude to my Dissertation Advisor **Dr. Mukesh Kumar**, Asst. Professor Electronics & Communication Engineering Department, Thapar University, Patiala for their continuous indefatigable guidance which paved me on to the part to carry this dissertation within time. I am highly indebted to them for their efforts and invaluable suggestion during the period of work.

I take this opportunity to express my gratitude and sincere thanks to **Dr. Sanjay Sharma**, Professor and Head, **Dr. Kulbir Singh**, Associate Professor of Electronics & Communication Engineering Department for their valuable advice and suggestion and for providing me the opportunity to complete my thesis work.

I would also like to thank all the staff member of Electronics & Communication Engineering Department for providing me all the facilities required for the completion of this work.

ABSTRACT

Conventional optical fibers can only guide light in a high refractive index core by total internal reflection. By using total internal reflections, it is not possible to guide light in an air core. Light guidance in air is of great interest for various technological and scientific applications and has only recently been possible with the advent of photonic band gap fibers. Control of dispersion in PCFs is very important problem for realistic applications of optical fiber communications, dispersion compensation and nonlinear optics. Usually the positive dispersion of the optical fiber, which is a major factor to cause optical pulse broadening and restrict transmission distance and bandwidth, can be compensated by using dispersion compensating fiber (DCF) with large negative dispersion.

The present work aims at the designing and simulation of a structure with high electric field distribution, low group velocity and low group velocity dispersion single mode photonic crystal fibers. By varying various parameters such as radius of air holes (r), number of air holes rings (N), dielectric constant of material (ε), and lattice constant (a) analysis has been done for an optimum profile. In ε=12, provides maximum electric field distribution and low group velocity dispersion in the largest possible wavelength window, in which the dispersion varies from -0.3420 to –1.1324 ps/nm/km, providing a group velocity 0.19c. For ε=7.84, flattened group velocity dispersion in a range of -0.2688 to -0.3536 ps/nm/km and group velocity 0.22c have been achieved. Largest negative group velocity dispersion ranging from -0.9875 to -0.5376 ps/nm/km has been achieved with ε=2.1, for which group velocity touched the value of 0.38c within the minimum wavelength window of 0.59 to 1.00μm.

LIST OF TABLES

LIST OF FIGURES

CHAPTER 1

INTRODUCTION

1.1 Background

Photonic crystal fibers are also known as microstructure optical fibers having a microstructure in the transverse plane [1]. These fibers can guide light by means of total internal reflection, as in standard fibers, or by the photonic bandgap effect. There also exist fibers with a periodicity in the propagation direction of the light. Such fibers are called fiber gratings. The axial periodicity can induce coupling of light between co-propagating or counter-propagating modes.

1.1.1 Initial Developments of PCFs

At about the same time as the standard, step index fiber was developed [2], it was recognized that light could be guided in a silica core, surrounded by a microstructure air/silica cladding [3]. However, work on this type of fiber was abandoned due to the success of the step index fiber. In the mid-1970s, a new type of guiding mechanism was proposed and analyzed by Yeh et al. [4–6]. They considered light guidance by Bragg scattering from a periodic cladding. This allows for light to be guided in a hollow core. The new type of fiber, known as a Bragg fiber, did however prove difficult to fabricate. The proposal that light can be confined in all three spatial dimensions due to the photonic bandgap effect [7, 8], stimulated much interest in photonic crystals [9]. The idea of using a photonic bandgap to trap light inspired Knight et al. to stack silica capillaries together in a hexagonal lattice, and draw them to a PCF with a solid core [10]. The first PCF did however not guide light by the photonic bandgap effect. Instead, the air holes lowered the effective index of the periodic cladding, making the fiber guide light by total internal reflection [11]. An example of such an index-guiding PCF is shown in Fig1.1.

By optimizing the PCF structure, true bandgap guidance was then established in a hollow core PCF [12]. However, the guided light was mainly located in silica in this fiber. This was overcome by Cregan et al. in 1999, who experimentally demonstrated bandgap guidance in air [13].

Figure: 1.1 Cross-section view of an index-guiding photonic crystal fiber [73].

The first comprehensive theoretical analysis of air-guiding PCFs came shortly after [14]. It can be noted that there are several examples of photonic microstructures in nature. One example is the Morpho rhetenor butterflies, having highly reflective wings due to discrete multilayers of varying refractive index [15].

1.1.2 Applications of PCF

Photonic crystal fibers have created a number of applications. A review of some properties and applications of PCFs can be found in Refs. [16–18]. Since bandgap guiding PCFs can guide light in an air core, the guided light is little affected by the absorption of 0.15dB/km in silica. This suggests that air-guiding PCFs might find applications as transmission fibers.

However, other loss mechanisms must be taken into consideration [19]. The lowest loss demonstrated to date is 13dB/km in a single-mode air-guiding PCF [19], and 1.7dB/km in a weakly multimode air-guiding PCF [21]. The latter result is still about an order of magnitude larger than the loss of standard fibers.

Low loss alone is not sufficient for a successful transmission fiber; the effects of dispersion are also important for transmission at high bit rates. It has recently been shown theoretically that the waveguide dispersion of air core Bragg fibers can be tailored by introducing defects in the cladding [22]. Small-core index-guiding PCFs with high air fill fraction can have unusual dispersion properties in addition to high effective nonlinearity. Ranka et al. observed a broadening of the pulse spectrum when launching 100 fs pulses with 0.8nJ energy into a 75cm long PCF [23]. In fact, the wavelength spectrum of the pulse spanned over more than

one octave after propagation through the fiber. This broadening, called super continuum generation, is caused by the combination of dispersion and nonlinearity of the PCF. Supercontinuum generation has found applications within frequency meteorology [24]. PCFs equivalent to double-clad fibers are useful within the field of high power fiber lasers and amplifiers [25, 26]. This is due to the possibility of having an outer cladding with high NA, allowing for high pump collection efficiency, and a large, active, single-mode signal core, reducing nonlinear effects. Interesting physics and applications are found when filling the air holes with various materials. Low threshold stimulated Raman scattering has been demonstrated in a Hydrogen-filled air-core PCF [27]. Various devices, such as a variable optical attenuator has been demonstrated by filling the air holes of a solid core PCF with polymers [28]. Another interesting possibility is to fill the air holes of an initially index-guiding PCF with a high-index liquid. This will turn the fiber into a bandgap guiding PCF. Tunable bandgap guidance has been demonstrated in such a fiber by varying the temperature [29]. Filling the air holes with liquid crystals is particularly interesting, since they can be highly sensitive to external perturbations [30]. Finally, it must be emphasized that advanced fully-vectorial simulation programs are of prime importance in the design of PCFs, due to the complexity of the PCF structures.

1.1.3 Dispersion in Optical Fiber Links

In optics, dispersion is the phenomenon in which the phase velocity of a wave rest on its frequency, or otherwise when the group velocity depends on the frequency. Media having such a property are termed dispersive media [32]. Dispersion is sometimes known as chromatic dispersion to emphasize its wavelength-dependent nature or group-velocity dispersion (GVD) to emphasize the character of the group velocity. The maximum familiar example of dispersion is probably a rainbow, in which dispersion reasons the spatial separation of a white light into components of not the same wavelengths (different colors). However, dispersion also has an effect in a number of other circumstances: for example0, [33] GVD causes pulses to spread in optical fibers, degrading signals over large distances; also, a cancellation between group-velocity dispersion and nonlinear effects leads to soliton waves. Dispersion is finest often defined for light waves, but it may occur for some kind of wave that interacts with a medium or passes through an inhomogeneous geometry (e.g a

waveguide), such as sound waves. There are mostly two sources of dispersion: material dispersion and waveguide dispersion [34]. Material dispersion derives from a frequency-dependent answer of a material to waves. For example, material dispersion leads to undesired chromatic aberration in a lens or the parting of colors in a prism. Waveguide dispersion follows when the speed of a wave in a waveguide (such as an optical fiber) depends on its frequency for geometric reasons, independent of any frequency dependency of the materials from which it is constructed. More generally, "waveguide" dispersion can occur for waves propagating through any inhomogeneous structure (e.g., a photonic crystal), whether or not the waves are confined to approximately region. In general, both types of dispersion may be existent, although they are not sternly additive. Their mixture leads to signal degradation in optical fibers for telecommunications, for the reason that the varying delay in arrival time in the middle of different components of a signal "smears out" the signal in time [35].

1.2 Advances in Research of Photonic Crystal Fibers

Until recently, an optical fiber was a solid thread surrounded by a different material with a lower refractive index. Today the photonic crystal fibers (PCFs) are recognized as a different fiber technology. PCFs, which have been first established in 1995, are optical fibers with a periodic arrangement of low-index material in a background with higher refractive index. The background material in PCFs is usually undoped silica and the low index area is typically provided by air-holes running along their whole length. Two main categories of PCFs exist: high-index guiding fibers and photonic band gap ones. PCFs belonging to the first category are more similar to conventional optical fibers, because light is confined in a solid core by exploiting the modified total internal reflection mechanism. In fact, there is a positive refractive index difference between the core region and the photonic crystal cladding, where the air-hole existence causes a lower average refractive index. The guiding mechanism is defined as modified because the cladding refractive index is not a constant value as in standard optical fibers but it changes significantly with the wavelength.

This characteristic as well as the high refractive index contrast between silica and air provides a range of new interesting features. Moreover, high design flexibility is one of the distinctive properties of PCFs. In specific, by changing the geometric characteristics of the air-holes in the fiber cross-section, that is, their dimension or position, it is possible to obtain

PCFs with diametrically opposite properties. For example, PCFs with a small silica core and large air-holes, that is, with a high air-filling fraction in the transverse section have better nonlinear properties compared with conventional optical fibers and so they can be well used in many applications, like super continuum generation. On the different fibers can be designed with small air-holes and large hole-to-hole distances in order to obtain a large modal area, useful for high power distribution. Differently from standard fibers PCFs with proper geometric characteristics can be endlessly single mode, that is, only the fundamental mode is guided regardless of the wavelength. In addition a significant asymmetry can be introduced in a simple way in the PCF core, thus creating fibers with very high level of birefringence. Moreover the PCF dispersion properties can be tailored with great flexibility so that it is possible to move the zero-dispersion wavelength to the visible range as well as to obtain dispersion curves ultra-flattened or with a strong negative slope [37- 39].

When the PCF core region has a lower refractive index than the nearby photonic crystal cladding, light is guided by a mechanism different from total internal reflection by exploiting the presence of the photonic band gap (PBG). In fact, the air-hole microstructure which constitutes the PCF cladding is a two-dimensional photonic crystal that is a material with periodic dielectric properties characterized by a photonic band gap, where light in certain wavelength ranges cannot propagate. The PBG effect can be also found in nature since it is responsible, for example, of the beautiful and bright colors seen in butterfly wings. PCFs with a low index core are created by introducing a defect in the photonic crystal structure, for example, an extra air-hole or an enlarged one, and light is confined because the PBG makes propagation in the micro structured cladding region impossible. This guiding mechanism cannot be obtained in conventional optical fibers and it opens a whole different set of interesting possibilities. In particular, light can be guided in air in PCFs with a hollow core thus providing numerous promising applications such as low-loss guidance and high-power distribution without the risk of fiber damage. Moreover air-guiding PCFs are almost insensitive to bending even for small bending diameter values and they present extreme dispersion properties, highly dominated by the waveguide component. Finally, when filled with proper gases or liquids, hollow core PCFs can be successfully employed in sensor applications or for nonlinear optics.

The main drawback which affects this new kind of fibers is related to the attenuation, which is higher than that of conventional optical fibers. The different loss mechanisms are thus studied for both solid and hollow-core photonic crystal fibers. In general, a loss reduction for PCFs can be obtained by improving the fabrication process, reported in the last part of the chapter. The stack-and draw process is described with other fabrication techniques [40]. Once reached the technological maturity, the advantages offered by PCFs with respect to conventional fibers could be completely exploited for different applications and the new fibers will enter concretely in the market.

1.3 Outline of Dissertation

The present work aims at the designing a structure with high electric field confinement, low group velocity and low group velocity dispersion, single mode air photonic crystal fibers. In this work, several parameters are varied such as radius of air holes (r), number of air holes rings (N), dielectric constant of material (ε), dielectric constant analysis has been done for an best profile design. The simulation is done and results are validated with MIT photonic bands.

Chapter 2 Provides an introduction to photonic crystal fibers, as well as a description of the stack and draw technique used for the fabrication of silica photonic crystal fibers. It also takes in a comprehensive description of the optical properties of photonic crystals and the optical properties of index-guiding PCFs are briefly discussed.

Chapter 3 Discusses about the research work done in the photonic crystal fibers.

Chapter 4 Discusses the design and simulation of photonic crystal fiber with high electric field confinement, controlling of dispersion, low group velocity and low cladding loss.

Chapter 5 summarizes the whole dissertation with some closing remarks and presents the scope of photonic crystal fiber in near future.

CHAPTER 2

Characteristics & Applications of Photonic Crystal Fiber

2.1 Features of Photonic Crystal Fiber

It is important to indication that photonic crystal fibers are also referred as microstructure optical fibers. In a conventional optical fiber the light propagation is due to total internal reflection at the core/cladding interface. In contrast to this, PCFs are capable to guide light by means of two different mechanisms: Modified total internal reflection, in which light is guided in a solid core, surrounded by a structured cladding. In this case the average refractive index of the cladding is reduced because of the air holes (low refractive index) [41]. On the other hand, photonic band gap fibers exploit two dimensional photonic band gaps as the mechanism of light guidance therefore they can guide light in a low refractive index medium [42, 43, 44]. In photonic band gap fibers the air holes that define the cladding region are arranged in a periodic lattice which presents a photonic band gap that does not allow light to propagate in the cladding region under certain conditions.

A good starting point for understanding the properties of photonic crystal fibers is that of photonic crystals. This section gives an insight into photonic crystal and the formation of photonic band gaps. A complete review of the optical properties, guidance mechanisms and fabrication methods of photonic crystal fibers is also presented here.

In the previous year scientists and engineers have been concerned about controlling the optical properties of materials. We know of the conventional fiber-optic cables which simply guide light trough a glass core by the law of reflection. A fiber optic cable was discovery in data transmitting and they have revolutionized the telecommunication industry among others. With photonic crystals we assume to be able to control light in an optical fiber, even with core index lower than the cladding index, & both the theoretical and experimental research have been very promising so far. But what is a photonic crystal? From solid state physics we associate a crystal with a collection of atoms arranged in a certain lattice, and photonic crystals are nothing else than a periodic arrangement of dielectric media. Photonic crystals have a lot in common with traditional crystals and we can adopt many of the theories from solid state physics combined with electromagnetism when dealing with photonic crystals. In

fact photonic crystals can most have all be described as the optical analog to semiconductors with the electrons replaced by electromagnetic waves. By designing a given photonic crystal we can also create a frequency band gap where no electromagnetic waves are permitted. This band gap is one of the most essential features of the photonic crystal and with that they should be able to create many new and exciting devices such as optical printed circuit boards, new and improved fiber-optic cables and much more. Let us now take a closer look at the photonic crystals.

2.2 Fabrication of PCF

Optical fiber fabrication typically includes two stages, preform fabrication and fiber drawing. A preform is a large-scale replica of the fiber normally 50cm in length and 20mm in diameter (for PCFs). A preform is drawn down to micro-scale dimensions on a fiber drawing tower (see Fig. 2.1). During the comparatively short history of PCFs they are now made in many laboratories around the world using various preform synthesis methods, such as: stacking of capillaries and rods, sol-gel casting ultrasonic drilling [45], extrusion from bulk glass with low softening temperature and rolling flexible material sheets into tubes [46], each of which has advantages and disadvantages depending on the glass used and the desired fiber geometry.

For silica PCFs, capillary stacking has become the most widely used technique mainly due to the design flexibility it offers. In this approach, firstly, approximately half meter long capillaries with a typical outside diameter of 1mm are drawn from a starting tube of large purity synthetic silica with an outer diameter of 10-20mm. The inner/outer diameter of the initial tube determines the ratio between the hole diameter and the lattice pitch $(d/\wedge)$ in the drawn fiber. The capillaries are stacked on a horizontal ring in a close-packed arrangement which reproduces the structure that is to be obtained in the final fiber. These packages are then inserted into a jacket tube and packing silica rods of different diameters are carefully inserted to ensure mechanical stability of the structure. A rod placed in the center of the stack acts as the solid core of index-guiding PCFs and a tube is inserted if a hollow-core PBGF is to be achieved. The resulting PCF preform is then drawn down to canes of few millimeters diameter. The top end of the capillaries can be sealed in order to make pressure gradient to balance the collapsing effect of surface tension during drawing. Vacuum is normally used

during this step to prevent the capillaries from moving [46]. The resulting cane is inserted into a solid jacket tube and by applying a second drawing stage a PCF is produced. In this latest stage, the use of vacuum, pressure and the control of the drawing parameters (tension, furnace temperature, feed speed, fiber speed, etc.) are very important to obtain a fiber with best characteristics. Fig. 2.1 shows a summary of the stack and draw fabrication method. An amazing property of silica-air photonic crystal fibers is that the air channels in centimeter scale preforms are preserved when drawn down to the micro-scale. After drawing, these micrometer wide channels run along fibers that can be hundreds of meters of even a couple of kilometers long. During drawing the preform is mounted in a holding chuck attached to a feed mechanism that lowers the preform into a furnace at the feeding speed (Vp). The furnace temperature is raised above the glass-softening temperature about $1900^{\circ}C - 2200^{\circ}C$. As the glass softens a drop forms due to gravity [47]. The drawn fiber is taken up by the capstan which controls the draw speed (Vf). A variety of furnaces can be used to heat the preform. As turbulence around the fiber causes unacceptable variations in the fiber diameter, the furnace must provide laminar gas flow and must also give off no particles that might attach to the preform and degrade the fiber strength. The most common furnaces used that meet these requirements are graphite resistance and induction furnaces. The advantage of the induction furnace is its compact size compared to resistance furnaces. The furnace includes inert gas inlets to provide laminar flow of a sufficient quantity to maximize fiber strength and minimize diameter variations characteristic of turbulent gas flows. Furnace temperature is measured with an optical pyrometer from either the outer surface of the heating element or directly from the preform neck-down depending on the furnace set-up, the former being the more typical configuration. The temperature can be controlled to within $1^{\circ}C$. In order to maintain a uniform fiber diameter; the drawing process includes a diameter control loop. The fiber diameter is monitored as it exits the furnace. The output signal from the diameter monitor is used to automatically adjust the speed of the drawing capstan using a PID controller to obtain a constant diameter. Before the fiber reaches the capstan it is coated with a protective polymer. Coating is required to protect the pristine silica surface from scratches and abrasion and it preserves the intrinsic strength of silica. The coating usually consists of two layers of acrylate, a softer inner layer and a harder outer layer. However, it is possible to use the second coating only. Acryl ate coating is applied in liquid phase and is solidified by

UV-curing. Before coating the fiber must be cooled below 80◦ C. Thus, between the furnace and the coating cup the fiber is cooled down by the surrounding air. At high drawing speeds and with limited tower height it may be necessary to use [71] forced cooling using inert gases as helium. After coating the fiber passes over a capstan onto a fiber take-up that winds the fiber onto a spool. Prior to coating, the fiber surface is exposed to potential ambient contamination that will reduce the fiber strength. The fiber is therefore drawn in a clean room.

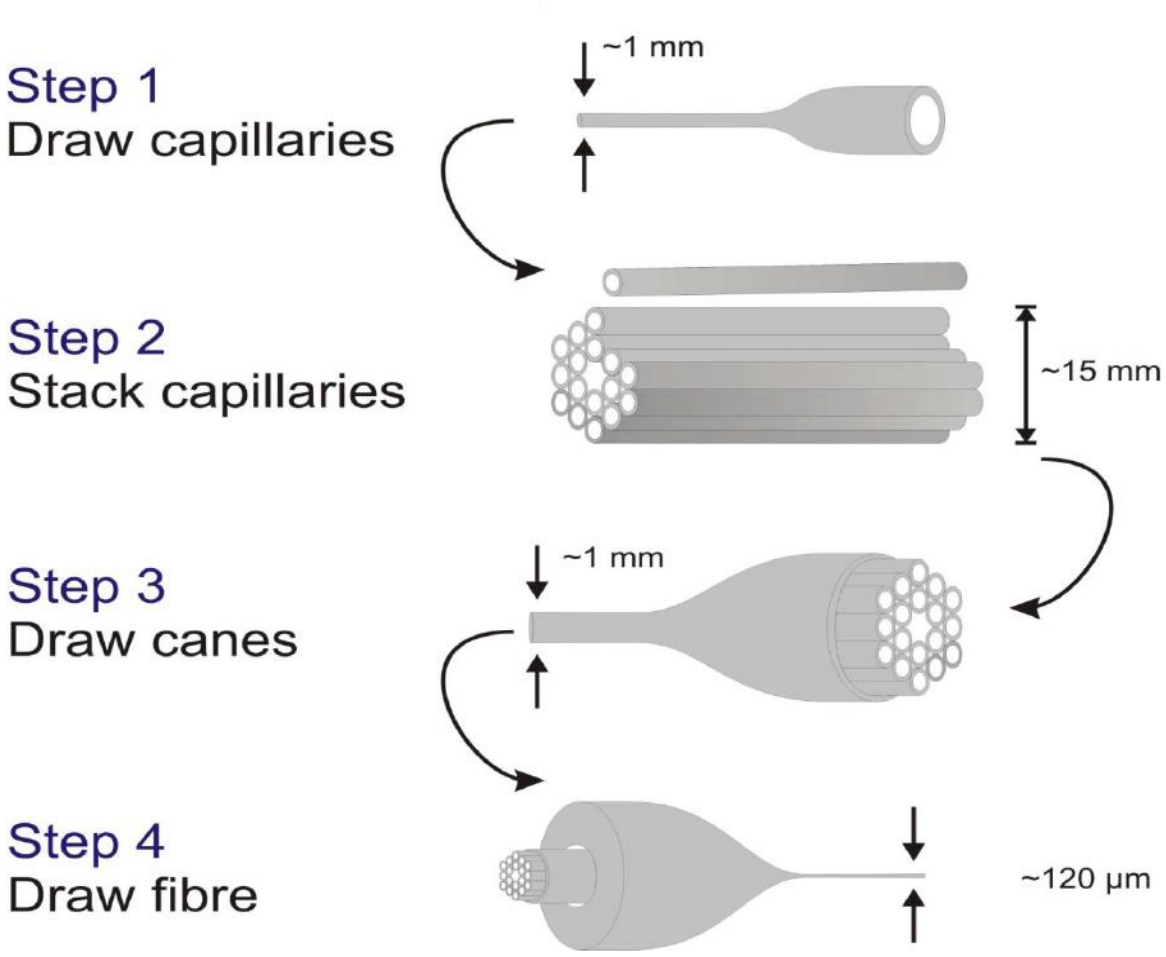

Figure: 2.1 Summary of the stack and draw PCF fabrication system. Silica capillaries and rods rawn and stacked in order to create a fiber preform. The preform is drawn down to a cane of 1mm and finally this cane is presented in a jacket tube and drawn down to a fiber [71-72].

The most important conduit for modern telecommunications is the optical fiber: a long filament of glass (or sometimes plastic) that guides light, often for a space of many

kilometers. Optical fibers are also used in a range of other applications, ranging from astrophysics to medicine. A traditional optical fiber consists of a central core that is surrounded by a cladding of slightly lower dielectric constant, which confines the light by index guiding. In this chapter, they will find that new regimes are opened for fiber operation by incorporating periodic structures in the cladding: photonic-crystal fibers.

2.3 Optical Confinement in Photonic Crystal Fibers

Photonic-crystal fibers, also known as micro structured optical fibers, can be divided into a few broad classes, according to whether they use index guiding or band gaps for optical confinement, and whether the periodicity of the structure is one-dimensional or two dimensional. Photonic crystal fiber confine light using a band gap rather than index guiding. Band gap confinement is attractive because it allows light to be guided inside a hollow core. This reduces the special effects of losses, undesired nonlinearities, and some other unwanted properties of the bulk materials that are available. Band-gap fibers with a one-dimensional periodicity a cladding with a series of concentric layers as in figure 2.2(a).were first analyzed precisely by Yeh et al. (1978), who known as Bragg fibers [48]. Band-gap fibers with two-dimensionally periodic claddings, as in figure 2.2(b), were described by Knight et al. (1998). The most commonly used design is a holey fiber, such as the one presented here, in which the cross section is a periodic array of air holes running the whole length of the fiber.

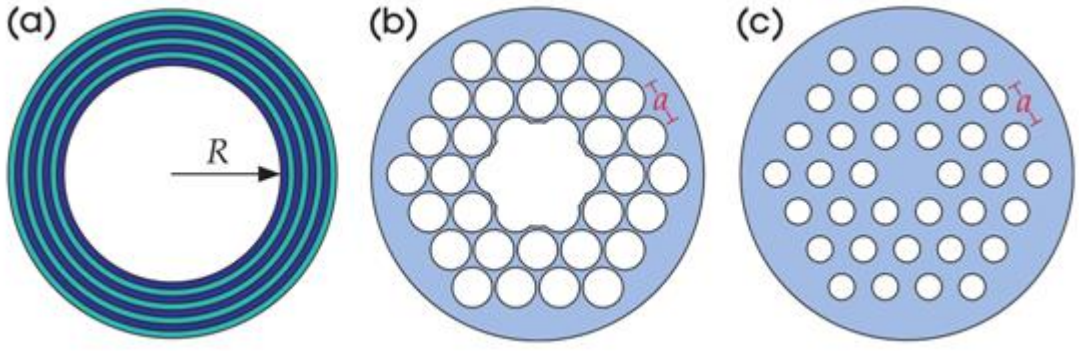

Figure: 2.2 Three models of photonic-crystal fibers. (a) Bragg fiber, with a one-dimensionally periodic cladding of concentric layers. (b) Two-dimensionally periodic structure with a triangular lattice of air holes, confining light in a hollow core through a band gap. (c) Holey fiber that confines light in a solid core by index guiding [71].

Another possibility is an index-guiding photonic-crystal fiber, in which the periodic structure is not working for its band gap, but rather to form an effective low-index cladding everywhere the core. One way to accomplish this is with a solid-core holey-fiber structure, as in figure 2.2(c). In this way, one can obtain a much higher dielectric contrast than is generally probable with solid fiber materials, leading to a better strength of optical confinement. This is often useful as a means of enhancing nonlinear effects, or of creating unusual dispersion phenomena.

Photonic-crystal fibers must an enormous practical advantage over the periodic structures that they discussed in previous: fibers can be created through a drawing process. In the first step of this process, a scale model of the fiber is created, typically centimeters in size. The preform is heated and pulled, stretching it like bubble gum into a thin strand whose cross section is a scaled-down version of the preforms. In this way, hundreds of meters or even kilometers of fiber can be drawn from a single preform, with near-perfect uniformity. They begin with index-guiding fibers, since those are the easiest to understand. They also demonstrate the important concept of the great frequency scalar limit, a rigorous asymptotic form of the Eigen modes that they use to describe many phenomena. Then, for photonic-bandgap fibers, they start with the example of two-dimensional periodicity and follow with one- dimensional periodicity. The reason for this reversal is not only that the holey bandgap fibers are closely related to their index-guiding counterparts, but also that Bragg fibers introduce some new concepts: continuous rotational symmetry and a new form of "tm" and "te" polarizations.

2.3.1 Index-Guiding Photonic-Crystal Fibers

The photonic-crystal fibers to understand are those that employ index guiding. They guide light by virtue of the smaller average refractive index of the cladding relative to the core [55]. A typical example is the holey fiber of figure 2.2(c), in which the cladding has a cross section that is a triangular lattice of air holes within an otherwise uniform dielectric medium. They use a spatial period a, with holes of radius 0.3a and a background dielectric constant of $\varepsilon = 3.4$ .The core is really just the position of a missing hole in the middle. One might optimism that it would be sufficient to consider only some average index contrast in the middle of core and cladding, but in fact a full understanding of this case requires an

analysis of the band diagram [48]. Since a fiber has translational symmetry along the fiber axis k_Z is conserved, and they can write the field in the usual Bloch form:

$$\boldsymbol{H}(x,y,t) = \boldsymbol{H}(x,y)\, e^{ik\, zz - i\omega t}$$

They design ω versus k_Z to obtain the band diagram (or dispersion relation), which is shown as an inset diagram in figure 2.3. The projected band diagram contains of two parts: a continuum of frequencies representing all of the possible extended states within the cladding, and a discrete set of guided bands with frequencies lying below the light cone. If the cladding material were uniform with a dielectric constant ε (independent of ω), then the light line would be a straight line, $\omega = ck_Z/\varepsilon$. For a no uniform cladding such as our lattice of holes, the light line is not straight. Instead, it is given by the fundamental space-filling mode of the cladding.

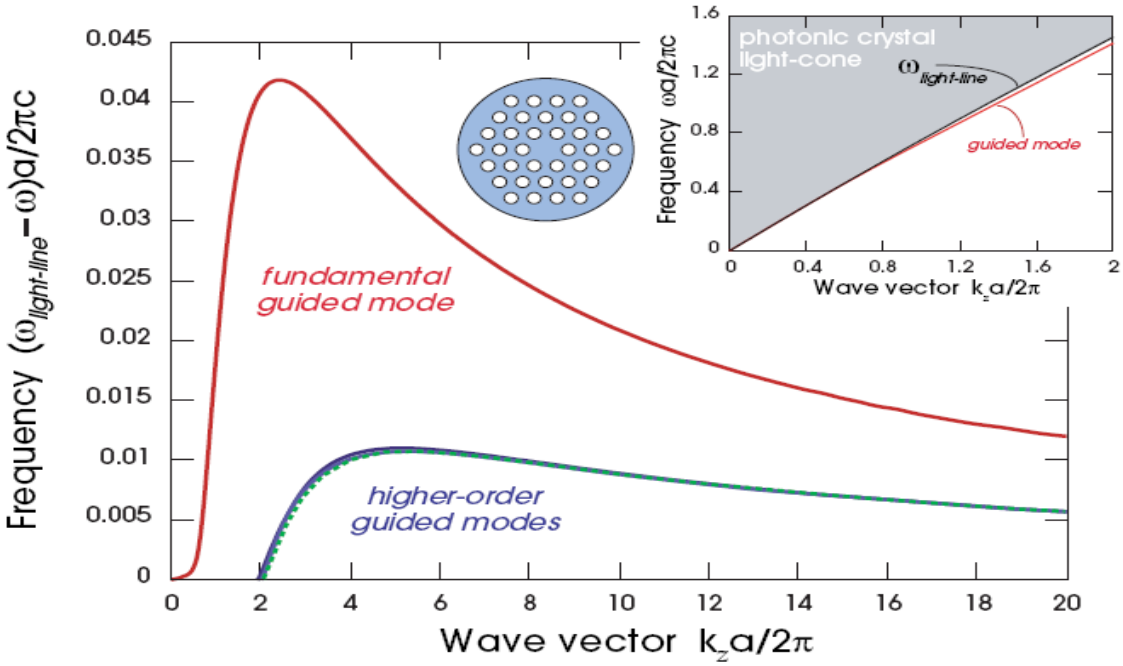

Figure: 2.3 Band diagram of solid-core holey fiber as a function of axial wave vector k_Z. The usual ω plot is inset, but for clarity they also plot the Δω between the guided bands and the light line. The higher-order guided modes are three bands that are nearly on top of one another [74].

In this structure, however, the guided mode is so close to the light cone that it is more convenient to plot the difference $\Delta\omega = \omega_{lc} - \omega$ between the light line ωlc and the guided band

ω, rather than plotting ω itself. This is done in figure 2.3. They have defined Δω such that it is positive for an index-guided mode. They can compute the light line in the same way they did previously when considering the continua of extended modes for linear defects or surface. For each k_z, they find all of the extended modes of the infinite periodic cladding for all possible transverse wave vectors(k_x, k_y). Then they design the resulting frequencies as a function of k_z. The lowest frequency for each k_z defines the light line. These extended modes are analyzed by considering the periodic cladding by itself: one need only consider (k_x, k_y) in the irreducible Brillouin zone of the triangular lattice.

The increased ε of the core presents one or more guided modes, by pulling down modes beneath the light line. Because they are below the light line, these modes must decay exponentially into the cladding. The farther below the light line they are pulled, the faster the transverse decay. For the case of figure 2.2(c), a doubly degenerate band is localized in the core, whose field patterns are shown in figure 2.4.

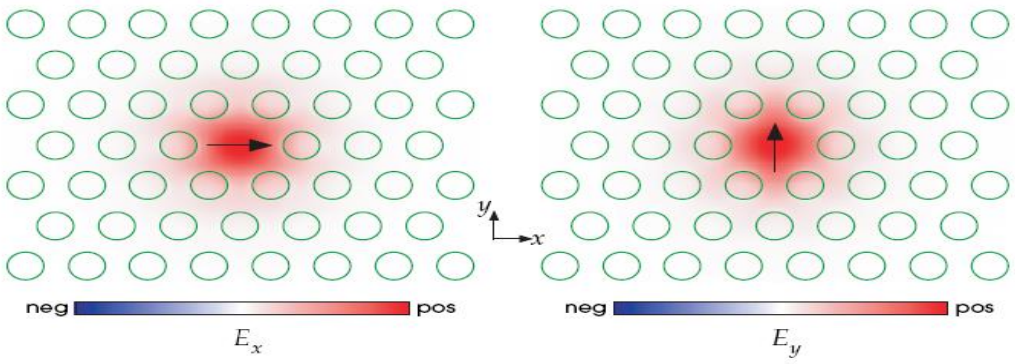

Figure: 2.4 Electric-field designs for the doubly degenerate fundamental mode of figure 2.3. Their polarizations are near orthogonal everywhere: the mode pictured at left is mostly E_x, and the mode pictured at right is largely E_y. The green rings show the locations of the air holes [48].

2.3.2 Band-Gap Guidance in Holey Fibers

Index guiding can be relied upon to confine light only within areas of higher effective index. In contrast, a photonic band gap can localize light in a waveguide with a lower index, such as the hollow core in figure 2.2(b). A fiber cannot have a complete band gap,

because of its continuous translational symmetry in the z direction, but a complete band gap is not necessary [72]. Because of the translational symmetry, the wave vector k_z is conserved, and it is therefore still suitable to have a band gap over some finite range of k_z. But how might such a gap arise in silica holey fibers such as those of the previous sections? And how can they use it to confine light in air?

2.3.3 Origin of the Band Gap in Holey Fibers

They begin by considering the periodic cladding by itself, without any core. At any specified k_z value, the results are the typical Bloch modes, comprising a band structure in a two-dimensional Brillouin zone. They would like to find a range of k_z for which the band structure has a gap in the middle of two bands.

Since they have a two-dimensionally periodic structure, our first desire might be to return to the results. Are the previously discussed two-dimensional gaps of any use here? The answer, unfortunately, is no, correspond to $k_z = 0$. In order to be useful in a waveguide, the gaps must extend over a range of nonzero k_z. If the crystal has a complete gap at $k_z = 0$, then indeed there will be a range of values of $k_z = 0$ over which the gap will persist. But the silica/air dielectric contrast of 3.4:1 is not sufficient to obtain such a complete two-dimensional gap .The silicon/air structure can have a TE gap, but not an overlying TM gap, and for $k_z = 0$ both the TE/TM distinction and the gap disappear [48].

What other recourse do they have to find a gap in a holey fiber? Since $k_z = 0$ was unhelpful, let us consider $k_z \to \infty$ instead. In this limit, as defined in the subsection The scalar limit and LP modes of chapter, the system is again equivalent to a two-dimensional system one in which the holes are replaced by perfect-metal rods and only an analogue of the TM polarization is present. Such a structure can indeed have a gap between two bands. They saw that a metallic rod radius of $r = 0.3a$ led to a gap between the second and third bands.

Furthermore, this band gap will appear not only for silica/air structures, but for any index contrast with the similar geometry, as long as they go to a high enough k_z. In this case, the first two "LP" bands in the scalar limit correspond to four vectorial modes, so they expect to see a gap open between the fourth and fifth bands for sufficiently large k_z.

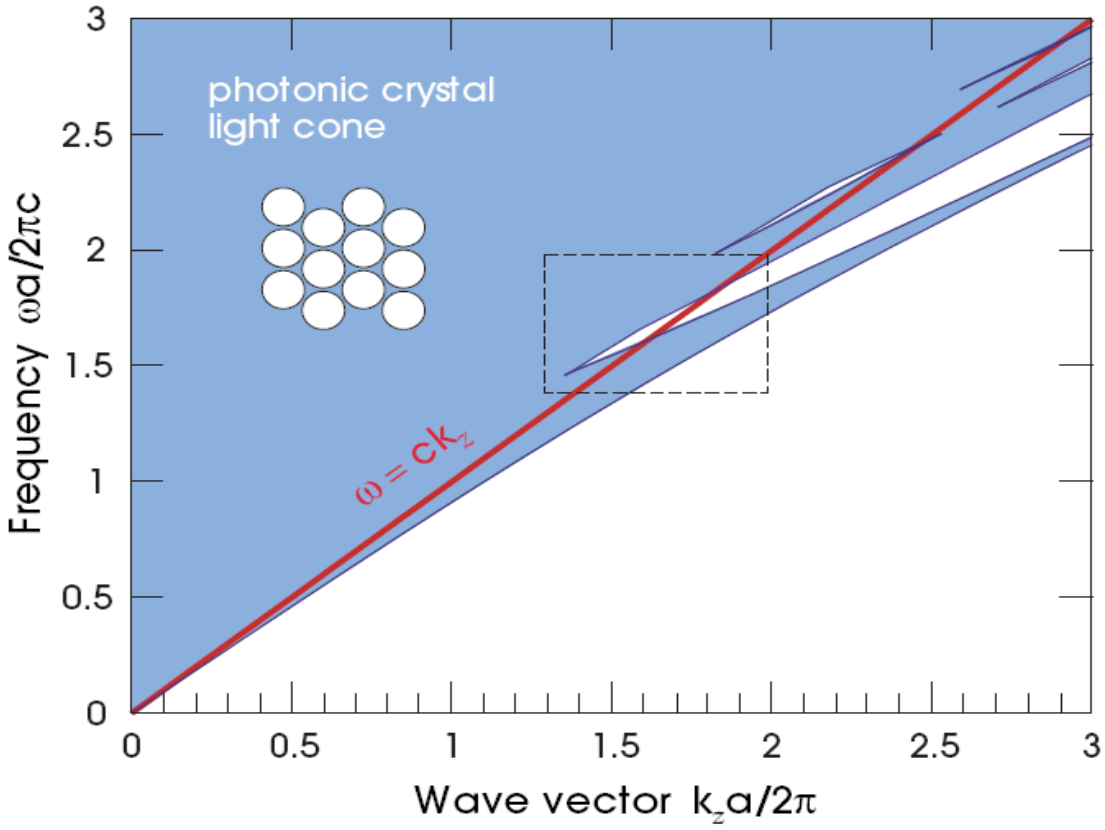

Figure: 2.5 Projected band diagram, as a function of out-of-plane wave vector k_z, for a triangular lattice of air holes in $\varepsilon = 2.1$. This methods the light cone of the holey fiber from figure 2.2(b), with gaps appearing as open areas. The light line of air, $\omega = ck_z$, is displayed in red [72].

As they will describe below, when guiding in an air core it is important that the gap open up when k_z is not too high, in order for the gap to extend above the light line of air ($\omega = ck_z$). Therefore, they rise the strength of the gap by enlarging the holes to r = 0.47a. The resulting projected band diagram is shown in figure 2.5, where they plot all the modes of this periodic cladding as a function of k_z. This is the light cone of the crystal, but unlike the light cone of a uniform medium it has openings above its lowermost boundary: the photonic band gaps. Just as they predicted from the scalar limit, the lowest gap is indeed between the fourth and fifth bands. This can be seen in the exact vectorial band diagram for the r = 0.47a holey fiber at a particular $k_z a/2\pi = 1.7$, shown in figure 2.6. There is, of course, a gap below the first band, corresponding to the index-guided region below the light cone, and the next gap is after the fourth band [74].

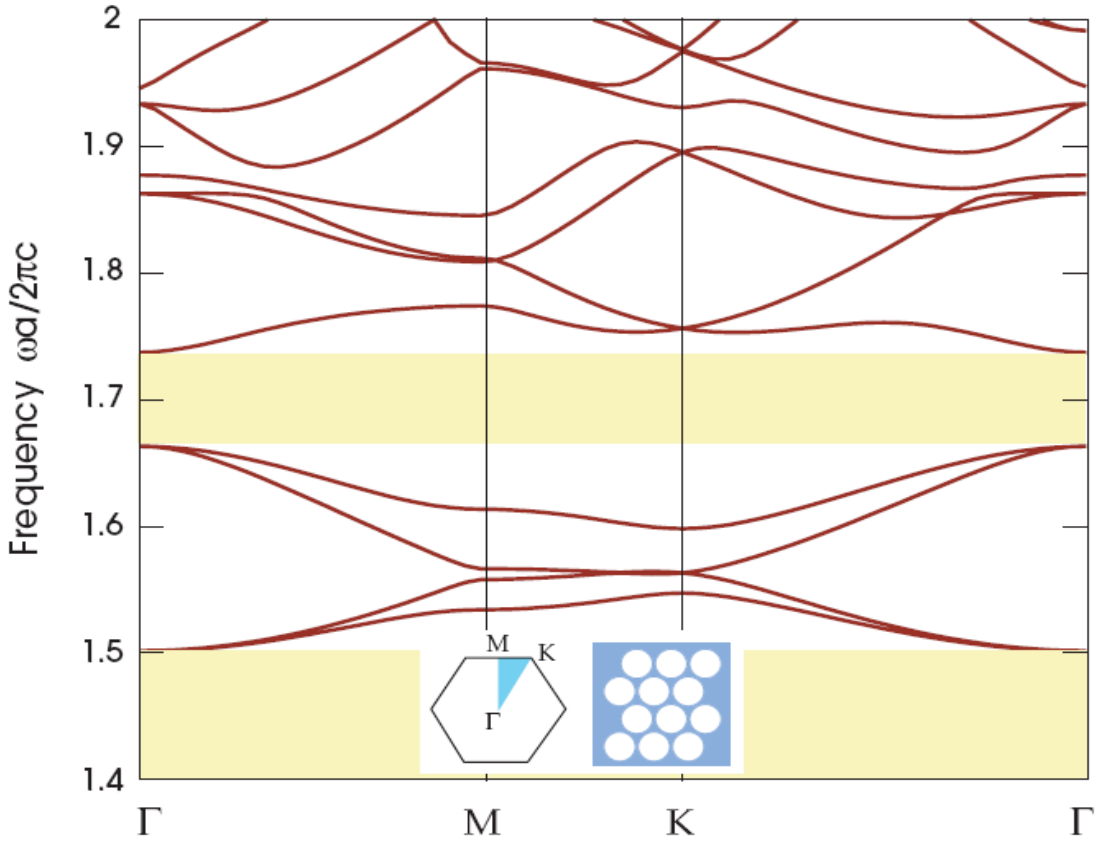

Figure: 2.6 Band diagram vs. in-plane wave vector in the irreducible Brillouin zone for the triangular lattice of air holes from figure 2.5, at an out-of-plane wave vector $k_z a/2\pi = 1.7$. Gaps are covered yellow: the lower gap corresponds to the index-guiding section, and the upper gap matches to one of the band gaps inside the light cone where guiding in an air core is possible [74].

2.3.4 Guided Modes in a Hollow Core

By now they are at ease with the proposition that, given a band gap, presenting a defect in the crystal can produce localized positions [48]. This phenomenon is demoralized to guide light in a hollow-core photonic-crystal fiber. Figure 2.7 shows the cross section of an experimental holey silica fiber with a hollow core cover the area of seven holes of the periodic structure. Theoretically, they will form a related cross section by enlarging a single hole to a radius of 1.202a, and they will focus on the modes within the first gap of figure 2.5 and exhibits a bewildering variety of guided modes. they can categorize these modes in two ways: by symmetry and by whether they are surface states or air-core modes.

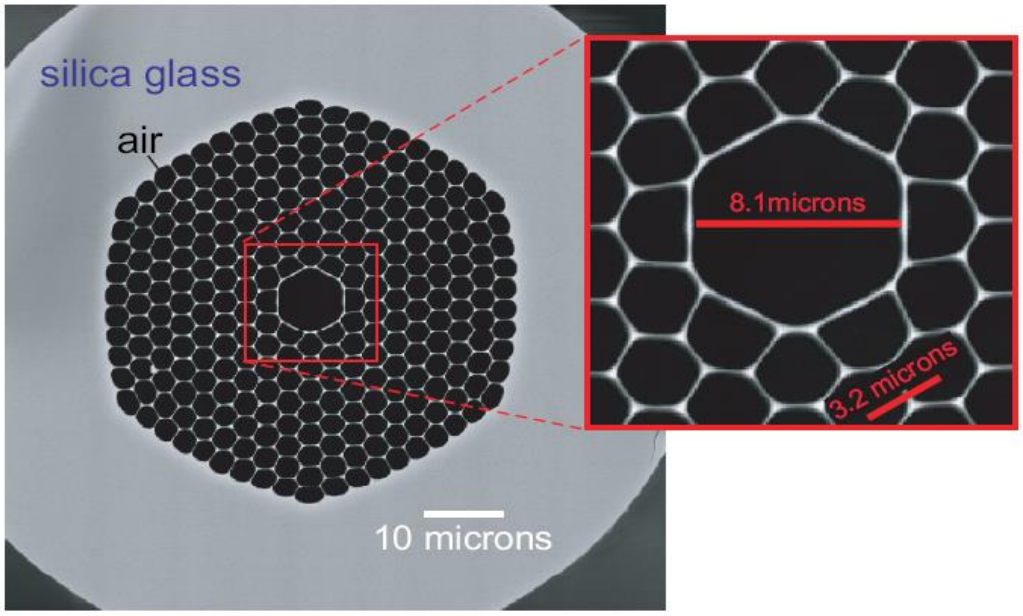

Figure: 2.7 Electron-microscope image of hollow-core holey-fiber cross section (black areas are air holes, and gray areas are silica glass).

2.4 Losses in Photonic Crystal Fibers

Optical fibers are used to transference light over distances ranging from meters to thousands of kilometers. Over such spaces, even small imperfections can lead to substantial effects. Conventional silica fibers have attained such an amazing degree of perfection that their losses (only about 0.2dB/km at 1.55μm) are limited by a mixture of intrinsic material absorption and scattering from microscopic density fluctuations. At longer wavelengths, on the other hand, such as the 10.6μm large-power lasers used for various industrial and medical applications, silica and other common fiber materials are not transparent at all.

Interestingly, not all losses are bad. As they have seen, most of the proposed hollow-fiber designs have been multi-mode. They support multiple guided modes that propagate at different speeds. Unchecked this results in modal dispersion: since it is impossible to avoid exciting multiple modes, the differing velocities cause pulses to spread and information transmission to be scrambled. However, this problem is reduced in a hollow-core fiber by differential attenuation: some modes have much lower losses than others, and thus transmission in everything but the lowest-loss mode will be filtered out after propagation over a long distance.

2.4.1 Cladding Losses

Three main loss mechanisms are associated with the amount of field penetration into the cladding: material absorption, radiative leakage due to the finite crystal size, and scattering from disorder. All of these will tend to reduction as the core radius R increases [1]. They will show that they typically decrease asymptotically as$1/R^3$. Of these three loss mechanisms, the simplest one to analyze is material absorption. This can be defined by a small imaginary part iκ that is added to the real refractive index n. Because κn for transparent materials, one can obtain essentially exact results for the loss by starting with the Eigen mode of the loss less structure and employ-in perturbation theory, Equation tells us the imaginary change Δω in the frequency due to κ, and to obtain the loss rate per unit distance they compute $\Delta k_z = -\Delta\omega/v_g$ via the group velocity $v_g = d\omega/dk_z$. Letting α 2 Im Δk_z, this describes a decay $e^{-\alpha z/2}$ in the fields and $e^{-\alpha z}$ in the intensity. Combining these equations, the decay rate α due to a single absorbing material with a complex refractive index $n + i\kappa$ is [47]

$$\alpha = \frac{2\omega k}{v_g n} \quad Fraction\ of \int \varepsilon |E|^2\ in\ absorbing\ material$$

(For the case of many materials, one simply adds the α from each material). As a special case, if the field energy propagates entirely within the material with a group velocity $v_g = c/n$ as for a plane wave (neglecting material dispersion), then one obtains a bulk absorption loss. Therefore, a useful dimensionless figure of merit for a hollow-core fiber mode is the ratio α/α_0. this is called the absorption suppression factor, the factor by which loss is decreased due to the portion of light in air.

2.5 Dispersion Properties of Optical Fiber

In optics, dispersion is the phenomenon in which the phase velocity of a wave rest on its frequency, or otherwise when the group velocity depends on the frequency. Media having such a property are termed dispersive media [32]. Dispersion is sometimes known as chromatic dispersion to emphasize its wavelength-dependent nature or group-velocity dispersion (GVD) to emphasize the character of the group velocity. The maximum familiar example of dispersion is probably a rainbow, in which dispersion reasons the spatial separation of a white light into components of not the same wavelengths (different colors). However, dispersion also has an effect in a number of other circumstances: for example,

GVD causes pulses to spread in optical fibers, degrading signals over large distances; also [33], a cancellation between group-velocity dispersion and nonlinear effects leads to soliton waves.

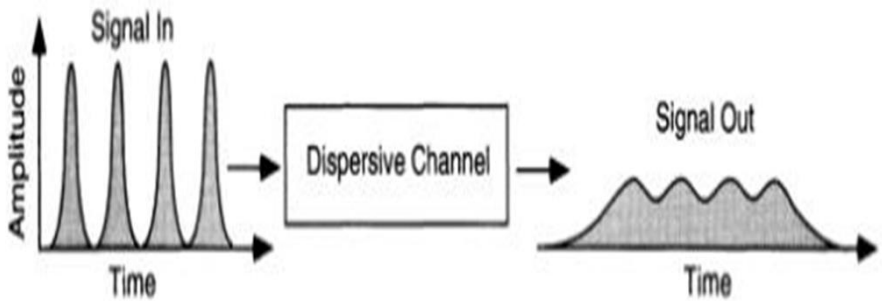

Figure: 2.8 Pulse Degradation from Dispersion in Photonic Crystal Fiber.

Dispersion is finest often defined for light waves, but it may occur for some kind of wave that interacts with a medium or passes through an inhomogeneous geometry (e.g a waveguide), such as sound waves [49]. There are mostly two sources of dispersion: material dispersion and waveguide dispersion. Material dispersion derives from a frequency-dependent answer of a material to waves. For example, material dispersion leads to undesired chromatic aberration in a lens or the parting of colors in a prism. Waveguide dispersion follows when the speed of a wave in a waveguide (such as an optical fiber) depends on its frequency for geometric reasons, independent of any frequency dependency of the materials from which it is constructed. More generally, "waveguide" dispersion can occur for waves propagating through any inhomogeneous structure (e.g., a photonic crystal), whether or not the waves are confined to approximately region. In general, both types of dispersion may be existent, although they are not sternly additive. Their mixture leads to signal degradation in optical fibers for telecommunications, for the reason that the varying delay in arrival time in the middle of different components of a signal "smears out" the signal in time.

2.5.1 Chromatic Dispersion (CD)

Chromatic dispersion is a broadening of the input signal as it travels down the size of the fiber. The concept to consider when talking about chromatic dispersion (CD) should be optical phase. It is important to indication optical phase before any explanations of CD or group delay because of their mathematical relationship. Group delay is defined as the first derivative of optical phase with respect to optical frequency [49]. Chromatic dispersion is the

second derivative of optical phase with respect to optical frequency. These quantities are represented as follows:

Group Delay = $\partial\varphi/\partial\omega$

Chromatic Dispersion = $\partial^2\varphi/\partial\omega^2$

Where φ = optical phase and ω = optical frequency

Chromatic dispersion consists of both material dispersion and waveguide dispersion as given away in Fig 2.9.

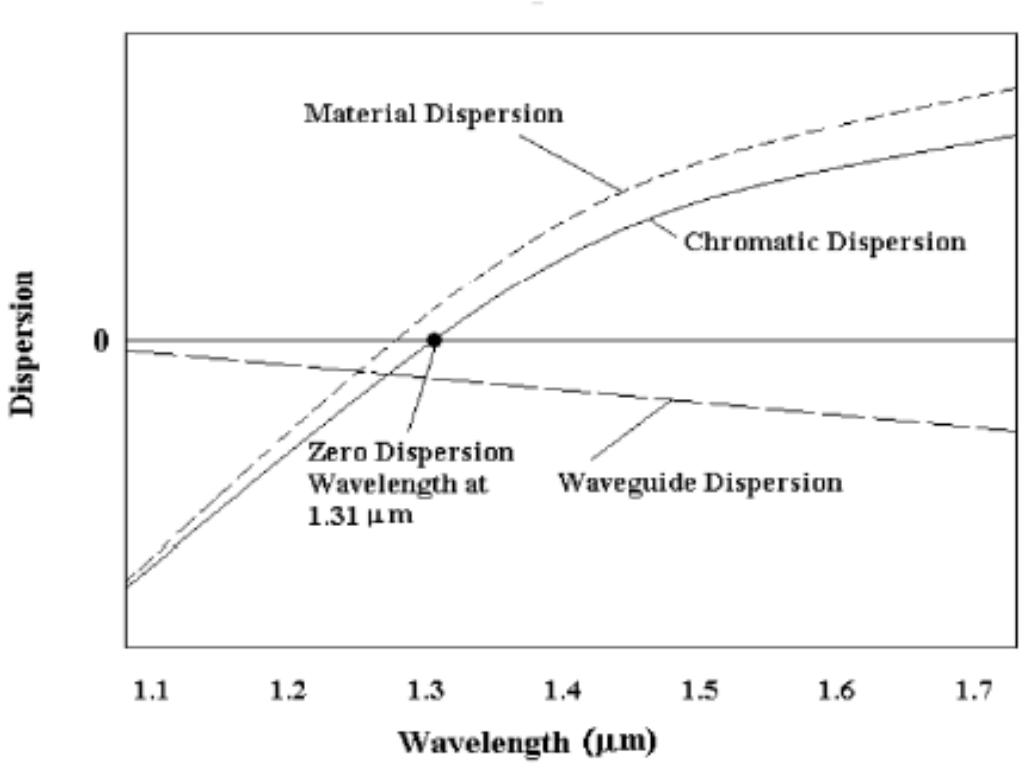

Figure: 2.9 Dispersion in a single mode optical fiber as a role of wavelength.

Both of these phenomena take place because all optical signals have a finite spectral width, and dissimilar spectral components will propagate at different speeds along the length of the fiber. One cause of this velocity difference is that the index of refraction of the fiber core is different for different wavelengths. This is known as material dispersion and it is the main source of chromatic dispersion in single-mode fibers. One more cause of dispersion is that the cross-sectional distribution of light within the fiber also changes for different wavelengths. Smaller wavelengths are more totally confined to the fiber core, while a higher

portion of the optical power at largest wavelengths propagates in the cladding. Then the index of the core is larger than the index of the cladding, this change in spatial distribution causes a change in propagation velocity. This phenomenon, shown in Fig. 2.10, is known as waveguide dispersion. Waveguide dispersion is relatively small compared to material dispersion [49].

Chromatic dispersion in a component is significantly different than chromatic dispersion in long length optical fiber. Chromatic dispersion remains constant over the bandwidth of a communications channel for long lengths of fiber. As a result, chromatic dispersion is a poor predictor of component performance in a communications system. Chromatic dispersion can cause bit errors in digital communications or distortion and a higher noise floor in analog communications, and can pose a serious issue in high-bit-rate systems if it is not measured accurately and some form of dispersion compensation is not employed.

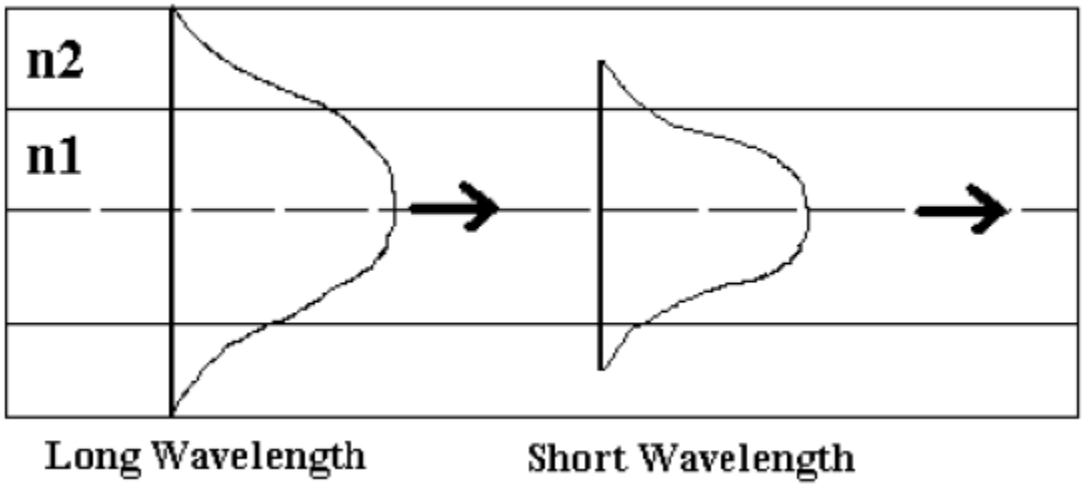

Figure: 2.10 Waveguide dispersion different wavelengths will experience different effective refractive index.

2.5.2 Group Velocity Dispersion (GVD)

A new consequence of dispersion manifests itself as a temporal effect. The formula $v = c / n$ calculates the phase velocity of a wave; this is the velocity at which the phase of any one frequency component of the wave will transmit. This is not the same as the group velocity of the wave that is the rate at which changes in amplitude will transmit. For a homogeneous medium, the group velocity vg is linked to the phase velocity by (here λ is the

wavelength in vacuum, not in the medium). The group velocity vg is often thought as the velocity by which energy and data is conveyed along the wave. In maximum cases this is true, and the group velocity can be assumed of as the signal velocity of the waveform. In some unusual circumstances, called cases of anomalous dispersion, the rate of change of the index of refraction with respect to the wavelength changes sign, in which case it is probable for the group velocity to exceed the speed of light ($vg > c$). Anomalous dispersion happens, for instance, where the wavelength of the light is near to an absorption resonance of the medium. When the dispersion is anomalous, however, group velocity is no longer an pointer of signal velocity. Instead, a signal movements at the speed of the wave front, which is c irrespective of the index of refraction.[49]

Recently, it has become probable to create gases in which the group velocity is not only higher than the speed of light, but even negative. In these cases, a pulse can appear to exit a medium before it enters. Even in these cases, however, a signal travels at the speed of light, as demonstrated by Stenner [49]. The group velocity itself is usually a role of the wave's frequency. This results in group velocity dispersion (GVD), which causes a minor pulse of light to spread in time as a result of different frequency components of the pulse travelling at different velocities. GVD is often quantified as the group delay dispersion parameter:

$$D = -\frac{\lambda}{c}\frac{d^2n}{d\lambda^2}$$

If D is small than zero, the medium is held to have positive dispersion. If D is larger than zero, the medium make sure negative dispersion. If a light pulse is transmitted through a normally dispersive medium, the result is the higher frequency components travel slower than the lower frequency components. The pulse therefore becomes positively chirped, or up-chirped, increasing in frequency with time. Conversely, if a pulse travels through an anomalously dispersive medium, high frequency components travel faster than the lower ones, and the pulse becomes negatively chirped, or down-chirped, decreasing in frequency with time. The result of GVD, whether negative or positive, is ultimately temporal spreading of the pulse. This makes dispersion management extremely main in optical communications systems based on optical fiber, since if dispersion is too high, a group of pulses demonstrating a bit-stream will spread in time and merge together, rendering the bit-stream unintelligible. This limits the length of fiber that a signal can be sent down without

regeneration. One possible answer to this problem is to guide signals down the PCF at a wavelength where the GVD is zero (e.g., around 1.3–1.5μm in silica), so pulses at t.his wavelength suffer minimal spreading from dispersion—in practice, however, this approach causes more problems than it solves because zero GVD unacceptably amplifies other nonlinear effects (such as four wave mixing). A new possible option is to use soliton pulses in the regime of anomalous ispersion a form of optical pulse which uses a nonlinear optical effect to self-maintain its shape solitons have the practical problem, however, that they need a certain power level to be maintained in the pulse for the nonlinear effect to be of the right strength. Instead, the result that is currently used in practice is to perform dispersion compensation, typically by matching the fiber by another fiber of opposite-sign dispersion so that the dispersion effects cancel; such compensation is ultimately limited by nonlinear effects such as self-phase modulation, which interact with dispersion to make it very difficult to undo. Dispersion control is also important in lasers that produce short pulses. The overall dispersion of the optical resonator is a major factor in determining the duration of the pulses emitted by the laser. A pair of prisms can be arranged to produce net negative dispersion, which can be used to balance the usually positive dispersion of the laser medium. Diffraction gratings can also be used to produce dispersive effects; these are often used in large-power laser amplifier systems. Recently, an alternative to prisms and gratings has been developed: chirped mirrors. These dielectric mirrors are coated so that different wavelengths have different penetration lengths, and therefore different group delays. The coating layers can be tailored to achieve a net negative dispersion.

2.6 Group velocity

The group velocity of a wave is the velocity by which the total shape of the wave's amplitudes known as the modulation or envelope of the wave propagates through space. For example, imagine what happens if a stone is thrown into the central of a very still pond. When the stone hits the surface of the water, a round pattern of waves appears. It soon turns into a round ring of waves with a quiescent center. The ever expanding ring of waves is the wave group, within which one can discern individual wavelets of differing wavelengths traveling at different speeds. The longer waves travel quicker than the group as a whole, but they die out as they method the leading edge. The shorter waves travel more slowly and they

die out as they emerge from the trailing boundary of the group. The group velocity v_g is defined by the equation:

$$v_g = \frac{\partial \omega}{\partial k}$$

Where ω is the wave's angular frequency and k is the angular wavenumber. The function ω(k), which gives ω as a role of k, is known as the dispersion relation. If ω is directly proportional to k, then the group velocity is correctly equal to the phase velocity. A wave of any shape will travel undistorted at this velocity. If ω is a linear function of k, but not directly proportional ($\omega = ak + b$), then the group velocity and phase velocity are different. The envelope of a wave packet will travel at the group velocity, while the individual peaks and troughs within the envelope will move at the phase velocity. If ω is not a linear function of k, the envelope of a wave packet will become distorted as it travels. This distortion is directly linked to group velocity, as follows. Since a wave packet contains a range of different frequencies, the group velocity $\partial\omega/\partial k$ is a range of different values (because ω is not a linear function of k). Therefore the envelope does not move at a single velocity, but a range of different velocities, so the envelope gets distorted. See further discussion below [51].

2.7 Photonic crystal fiber for Sensing and Dispersion Control

Photonic crystal fibers have created a number of applications. A review of some properties and applications of PCFs can be found in Refs. [16–18]. Since bandgap guiding PCFs can guide light in an air core, the guided light is little affected by the absorption of 0.15dB/km in silica. This suggests that air-guiding PCFs might find applications as transmission fibers.

However, other loss mechanisms must be taken into consideration [19]. The lowest loss demonstrated to date is 13dB/km in a single-mode air-guiding PCF [19], and 1.7dB/km in a weakly multimode air-guiding PCF [21]. The latter result is still about an order of magnitude larger than the loss of standard fibers.

2.7.1 Optical Sensors

Sensing is thus far a relatively unexplored area for PCFs, although the opportunities are myriad, spanning many fields including environmental monitoring, biomedical sensing, and

structural monitoring [47]. Multicore PCF has been used in bend and shape sensing and Doppler difference velocimetry double-clad PCF in multiphoton fluorescence measurements in medicine and solid-core PCF for hydrostatic pressure sensing.

2.7.2 Dispersion Compensation

The large glass air refractive-index difference makes it possible to design and fabricate PCFs with high levels of GVD. A PCF version of the classical W-profile dispersion compensating fiber was recently reported, offering slope-matched dispersion compensation for SMF-28 fiber at least over the entire C-band. Dispersion values of −1200 ps/nm/km imply that only 1 km of fiber is needed to compensate for 80 km of SMF-28. The fiber was made deliberately birefringent to allow control of polarization mode dispersion [47].

2.7.3 High-Power and Energy Transmission

PCF's ability to remain single mode at all wavelengths where it guides, and for all scales of structure, suggests that it should have superior power-handling properties the core area can be increased without the penalty of introducing higher order guided modes. The ability to transmit much higher power in a single mode has a major impact in the field of laser machining and high-power fiber lasers and amplifiers. The key issue is bend loss, and as they have seen, it turns out that PCF offers a wider bandwidth of useful single-mode guidance than high-Δ SMF, because it can operate in the multimode regime of SMF while remaining single mode (Section VI-B1). This also allows the long-wavelength bend edge to be moved to longer wavelengths. Hollow-core PCF is also an excellent candidate for transmitting high continuous-wave power as well as ultrashort pulses with very high peak powers. Solitons have been reported at 1550 nm with durations of 100 fs and peak powers of 2 MW and at 800 nm using a Ti:sapphire laser. The soliton energy is, of course, determined by the effective value of γ and the magnitude of the anomalous GVD. The GVD changes sign across the band gap, permitting choice of normal or anomalous dispersion, depending upon the application [47]. Further studies explore the ultimate power-handling capacity of hollow-core PCF.

CHAPTER 3

LITERATURE SURVEY

Ardavan F. Oskooi, *et al.* in 2009 [1] Present a holey photonic-crystal fiber with chalcogenide-glass index contrast can be calculated to have a complete gap at a propagation constant $\beta = 0$ that also extends into the **non**-zero β region. This type of bandgap opens up a regime for guiding zero–group-velocity modes not possible in holey fibers with the more common finger-like gaps originating from $\beta \rightarrow \infty$. Such modes could be used for hollow-core fibers in gas-sensor applications.

M.J. Gander, *et al.* Present a measurement of group velocity dispersion in photonic crystal fiber using low coherence techniques in 1999 [49]. The results verify theoretical predictions that photonic crystal fiber, unlike conventional step-index fiber, can display anomalous waveguide dispersion while remaining single mode. This allows the design of single mode fibers with zero dispersion points at wavelengths much shorter than is possible in standard fiber.

In 2013 [53] Abdelaziz, *et al.* Proposed by using a great birefringence and an ultra-flattened chromatic dispersion over a large wavelength range are achieved. It is shown that a low confinement loss can be obtained while the birefringence remains the same. The numerical results show that the presented PCF structure can be successfully employed as maintaining polarization devices working in a large zero- chromatic dispersion region.

Saeed Olyaee, *et al.* in 2011 [70] discussed highly suitable transmission media for optical communication systems. Small confinement loss, large effective area in a wide range of wavelengths, and ultra-flattened dispersion of PCFs is extremely desirable. In this paper, simulate a new structure of dispersion flattened photonic crystal fiber (DF-PCF). Also, investigate the tolerance analysis of the PCF deformations including tolerances of the pitch size and outer air holes diameter.

In 2006 [54] Yin Wang, *et al.* Present an Up to 14-ns delay is achieved by the SBS slow light in a 25-m long high nonlinearity photonic crystal fiber. The high delay efficiency improves the control rate of SBS slow light systems.

Michela Svaluto Moreolo, *et al.* in 2008 [51] Present a slow-light PhC structures based on the coupling of point defects. The performances of different enhanced coupled cavity waveguides are analyzed by using the tight binding (TB) approximation and the plane wave expansion (PWE) method. They show that light can be further slowed down by coupling high-Q cavities and that the delay line performance depends on the cavity symmetry. A group velocity of about 10^{-4} *c* can be reached and the bit length is 300 times smaller than the corresponding parameter of a fiber delay line.

Jan Sporik, *et al*. discussed Principle of PCF and its application in 2011 [55]. Simulations of one dimension photonic crystal are made. Possibilities of conventional fibers are shown and the comparison with PCF is done. Many types of commercially available PCF are listed. The Photonic Crystal Gaps are calculated for various one dimension periodic structures. Plane wave expansion method is used. The results are found by solving the eigenvalue problem for the intensity of Electric field. The influence of Photonic Crystal Gap on the layer width and the parameter gap-midgap ratio is discussed. The scalar solution for one dimension photonic crystal is found.

G.Calò, *et.al* in 2005 [69] introduced Photonic crystal fibers exhibit physical features, from various angles, more versatile, intriguing and promising than those pertaining to the conventional optical fibers. Their cross-section can be optimized to obtain single mode operation on a wide wavelenght range, soliton propagation, regeneration application, controllable group velocity dispersion. Moreover their core can be rare-earth doped so obtaining high-performance optical amplifiers and lasers or active components for optical communication systems.

In 2000 [56] J. C. Knight, *et al.* present the measured group-velocity dispersion characteristics of several air-silica photonic crystal fibers with anomalous group-velocity

dispersion at visible and near-infrared wavelengths. The values measured over a broad spectral range are compared to those predicted for an isolated strand of silica surrounded by air. They demonstrate a strictly single-mode fiber which has zero dispersion at a wavelength of 700 nm.

Marzena M. Tefelska, *et al.* in 2012 [68] discussed a measurement of the temperature dependence of the zero dispersion wavelengths in an air/silica photonic crystal fiber. This is done through a fourth-order four-wave mixing process by pumping the fiber in a low normal dispersion regime. The zero dispersion wavelengths are found to increase by about 10 nm from room temperature to 250 °C. This result is in good agreement with numerical simulations which demonstrate that it is mainly due to the thermo-optic effect. They found that the zero-dispersion wavelength evolution is not linear with temperature and that the shift rate is continuously increased from 39 pm/°C at room temperature to 63 pm/°C at 250°C.

Marzena M. Tefelska, *et al.* in 2012 [58] Present a very large mode area multimode photonic band-gap (PBG) propagation in a solid core photonic crystal fiber (PCF) filled with a liquid crystal (LC). The host fiber was designed with a 50-μm core diameter to optimize the light coupling from standard multimode fibers. After filling it with LCs, multimode selective propagation was observed and it was possible to tune the bands with temperature. The mode field was well localized in the core area and compared to our previous works, a much smaller percentage of optical power penetrates the LC-filled holes. Consequently, the scattering loss is reduced, allowing for lower insertion losses. Attenuation was measured by the cut-back technique and for one of the band gaps it was 0.16 dB/cm, which, to the best of our knowledge, has been the lowest level of attenuation reported so far in PBG-guiding LC-filled PCFs.

In 2012 [59] Yani Zhang, *et.al* Proposed a novel of photonic crystal fiber (PCF). Which is composed of a central defect core and cladding with elliptical air-holes along the fiber length. And two circle air-holes is enlarged in the near to central region to reduce core size and induce higher nonlinear. Its dispersion, birefringence and nonlinearity coefficient are investigated simultaneously by using the full vectorial finite element method. Mathematical

results indicate that the proposed fiber has two zero dispersion wavelengths and high birefringence high nonlinear effects, which will have important application in four-wave mixing and higher-order dispersion effects.

Ran Gao, *et.al* discussed a novel method for the measurement of chromatic dispersion (CD) profiles of photonic crystal fibers (PCFs) by using a tip interferometer is presented in 2013 [61]. A PCF tip interferometer is formed by splicing a short section of the PCF to a single mode fiber. The CD coefficient of the PCF is measured from 1525 to 1565 nm by using the white-light interferometry. The result of the proposed method agrees with that of the conventional swept wavelength interferometry. The maximum variation is only0.084 ps/nmkm at the wavelength of 1537.672 nm.

Jianhua Li, *et al*. in 2013 [62] Present very highly birefringent PCF with hybrid cladding is proposed. The birefringence is theoretically investigated with variant structural parameters and refractive index of filled material. The results show that the proposed PCF can provide high birefringence and be well tuned. It can be used as polarization controllers or sensors.

S. M. Abdur Razzak, *et al.* introduced an optimum design for highly nonlinear dispersion managed photonic crystal fibers in 2008 [63]. According to simulation, an eight-ringed photonic crystal fiber can be designed with a high nonlinear coefficient at 1550 nm with simultaneously flatter dispersion characteristics and low confinement losses. This fiber also assumes a high birefringence and has a modest number of design parameters.

In 2007 [64] Tim Birks, *et al.* Present tapering of photonic crystal fibers to make all-fiber mode converters for the LP11 and LP02 modes. The devices rely on adiabatic propagation rather than resonant coupling, allowing high extinction across a wide wavelength range.

Philip St.J. Russell, in 2006 [47] Present the history, fabrication, theory, numerical modeling, optical properties, guidance mechanisms, and applications of photonic-crystal fibers are reviewed.

Desmond M. Chow, *et al.* in 2012 [65] discussed the Fabrication of High Index Guiding Photonic Crystal Fiber is demonstrated using stack-and-draw technique. Fabricated Photonic Crystal Fiber has core size of 5.77μm and displays low loss single-mode guiding in communication band.

In 2013 [66] Assaad Baz, *et.al* Present the theoretically and experimentally analyze the benefit of hetero-structured cladding in Solid-Core Photonic Band Gap fibers so as to increase the loss ratio between high order modes and fundamental mode. When designed to operate in the 4*th* BandGap, a new design is proposed which permits to obtain mode field diameter of 44 whereas, for operation in the 3*rd* BandGap, a mode field diameter of 33 is obtained with 20 cm bending radius.

P**.** AndrCs, *et al.* in 2002 [67] Present a Systematic knowledge of the particular guiding properties of photonic crystal fibers (PCF's) permits the achievement of structures with flattened, or even ultra-flattened, positive, negative, or nearly-zero group velocity dispersion for different wavelength ranges. On the other hand, they have identify a PCF, called super-square PCF, in which the introduction of an off-lattice hole generates a highly anisotropic intrabaod guidance, and then the structure operates as a polarization maintaining fiber.

CHAPTER 4

Design For High Optical Confinement And Low Group Velocity

4.1 Structure of Photonic Crystal Fiber

Design of PCF consists of a solid core of material with a periodic array of air holes running along the length of the fiber acting as the cladding. In this kind of PCF the mean cladding refractive index is lesser than the core index. This type of fiber works on the principle of modified total internal reflection. In particular, design and construction of photonic crystals can be done with photonic band gaps that prevents light from propagating in certain directions with specified frequencies (i.e., a certain range of wavelengths, or colors, of light). As the operation is based on modified total internal reflection, the properties of high index core triangular PCFs in many respects resemble those of step index fibers [41].

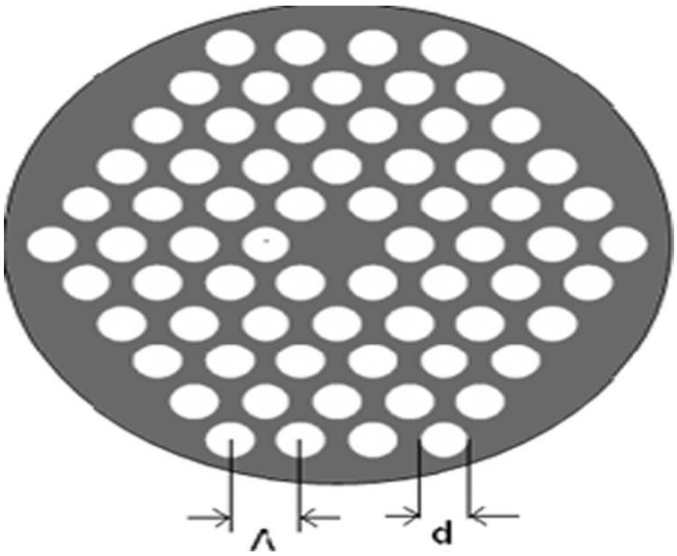

Figure: 4.1 photonic crystal fibers with a triangular lattice of air holes, where d is the hole diameter, ∧ is the pitch, and the dielectric constant of material (ε). In the center, an air hole is omitted creating a central high index defect serving as the fiber core.

The cross-sectional view of the proposed PCF design is shown in Fig 4.1. The cladding of the PCF consists of a square lattice of circular air holes with a radius (r). In the Centre, an air hole is omitted creating a central high index defect serving as the fiber core.

The proposed PCFs may not be simple to fabricate. However, the current movement in PCF technology has demonstrated that fabrication of even more complex PCF structures is possible. The possible errors during the fabrication process, as in any PCF structure, could affect the group velocity & group velocity dispersion. Fabrication error possibilities, such as the variation of hole size and hole-to-hole spacing (between.20a–90a) a is lattice constant. Our simulations results have indicated that, Fraction of Electromagnetic Energy is rather sensitive when air hole size and the position of inner rings are changed. A PCF can be considered as a two-dimensional waveguide that is periodic in X and Y directions. This PCF includes an array of dielectric rods. The light is assumed to propagate mostly along the Z axis and parallel to the rods. An important parameter should be considered for PCF designing is the group velocity dispersion [49]. It can be calculated from:

$$\boldsymbol{GVD} = \frac{\boldsymbol{\partial}}{\boldsymbol{\partial\omega}} \frac{\mathbf{1}}{\boldsymbol{v_g}} = \frac{\boldsymbol{\partial}}{\boldsymbol{\partial\omega}} \left(\frac{\boldsymbol{\partial k}}{\boldsymbol{\partial\omega}}\right) = \frac{\boldsymbol{\partial^2 k}}{\boldsymbol{\partial\omega^2}}$$

Where vg is group velocity, ω is the frequency and k is propagation constant.

Basic working of PCF does depend upon two modes, namely single mode and multi-mode. In multi-mode PCF instead of core the light is confined in both core and cladding due to the effect of hole pitch, diameter of air holes and the number of layers of air holes. Propagation of electric field distribution in multi-mode PCF has been shown in Fig. 4.2. But due to certain difficulties the multi-mode provides undesired results in the photonic crystal fiber case.

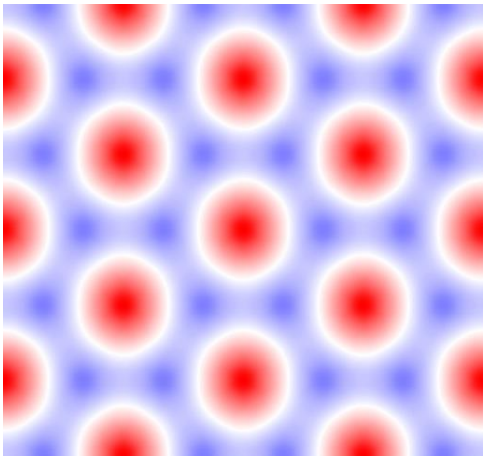

Figure: 4.2 Electric field distribution in multi-mode photonic crystal fibers.

The defect in the center acting as the core disturbs the periodicity of holes that helps in obtaining solid optical confinement in the core as shown in the Fig. 4.3. The periodic structure (air holes) surrounding the defect core causes a collective cancellation of scattering of light leading to localization of light in the defect region. Fig. 4.3 shows a strong optical confinement in defect core where N= 4×4, ε=12, r=0.42*a* (*a* is lattice constant).

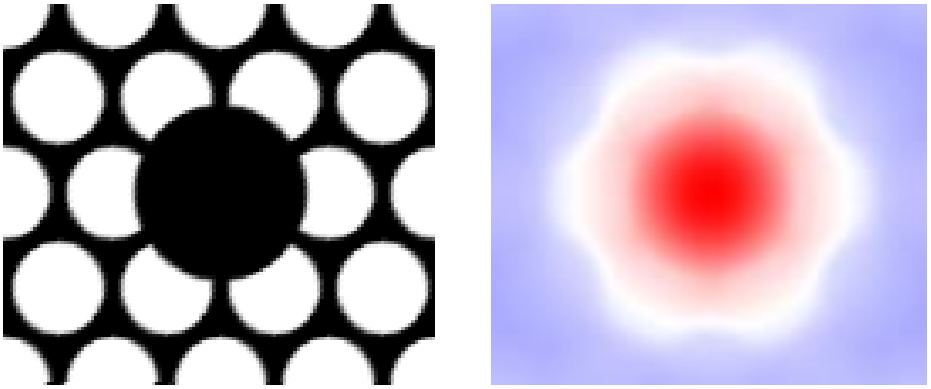

Figure: 4.3 Electric field distribution in the single mode photonic crystal fiber with core defect radius = 0.70*a*, N= 4×4, ε=12, r=.42*a*.

In single mode PCF light is totally confined in the core enabling various advantages such as low confinement loss, low scattering, low dispersion loss, low bending loss when compared with multi-mode PCF. Due to above qualities, single mode photonic crystal fibers have been taken into account in this thesis report. Fig. 4.3 represents the propagation of electric field distribution in single mode PCFs.

The defect described in figure (4.3) is just one out of many localized defect states, and by varying the radius of the crystal defect we can obtain other defect states. In order to use the defect states in practical applications, it is of great importance to know for which radius of the crystal defect, localized states exist. We have therefore plotted the fraction of electromagnetic energy inside the solid core defect as function of the defect radius. From figure (4.4) we see that the maximized localization happens for a defect radius of 0.70*a*. For this value 99% of the field energy is localized within the core-defect. Then the defect radius should be in the range [0.20*a*; 0.90*a*]. This means that we can adjust the lattice constant to make the band gap fit the demands on the operating frequency and construct the structure

which has largest confinement to the core-region. Until recently there have been some difficulties in fabricating solid core photonic crystal fibers with a defect radius within such a narrow range. In figure (4.3) we have plotted the field distribution of some structures from figure (4.4). From figure (4.4) we notice that the confinement fraction falls abruptly between the defect radius of 0.30*a* and 0.90*a*.

4.2 Effects of Different Parameters on Photonic Crystal Fiber:

4.2.1 Variation in Fraction of Electromagnetic Energy versus Radius of Core Defect at Different Material:

Fig. 4.4 shows the variations of electromagnetic energy of PCF with the radius of core defect (r) for various values of dielectric constant (ε). It can be concluded that electromagnetic energy increases as Radius of core defect increases as a whole. For low values of, Radius of core defect periodicity effect doesn't support its function, as fluctuations can be observed for hole radius values of 0.30*a* to 0.60*a*. As the core radius reaches value of 0.70*a* and above electromagnetic energy is almost constant & 99% as periodicity truly define its purpose thereafter.

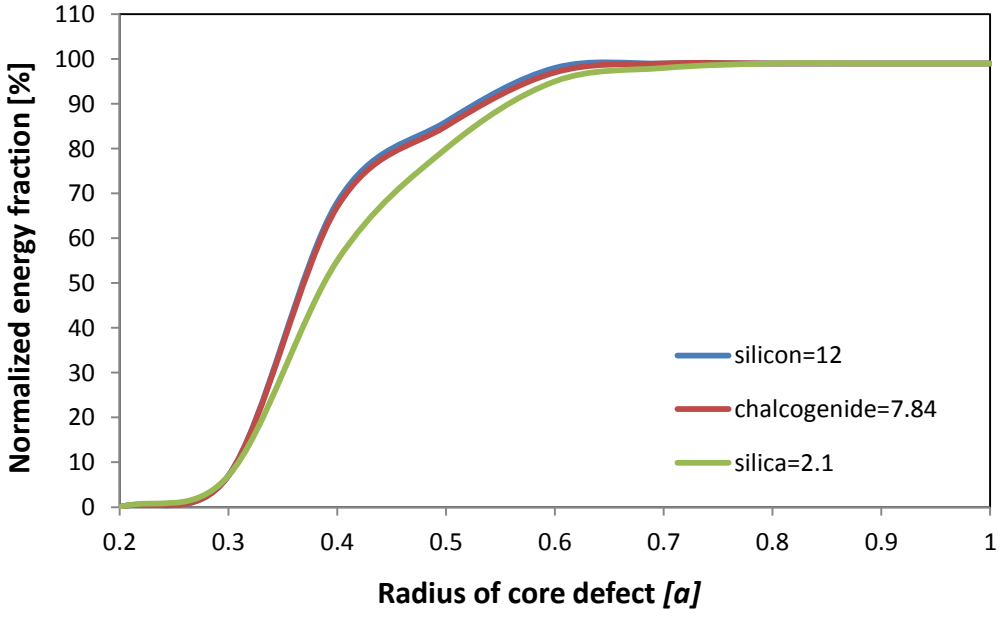

Figure: 4.4 The fraction of electromagnetic field energy localized inside the core-defect. The defect radius is varied between 0.20*a* and 0.9*a*. The size of the super-cell is 4 × 4 of the unit cell and holes radius 0.42*a*, lattice constant *a* =1.

A solid core is formed by removing some dielectric material, and here we do so by a cylinder-shaped solid core with an inscribed-circle radius r. The different types of modes with varying symmetry and degrees of confinement can be localized in fig (4.5). It has been proposed a four ring PCF with different dielectric constant and hole radius 0.42*a*, lattice constant = 1 for all the graph. In Fig 4.4 with hole radius=0.42*a*, & dielectric constant (ε) 12 provides maximum field energy in the largest possible defect radius 0.70*a* in which the field energy varies from 0% to 99%. For hole radius=0.42*a* and dielectric constant 7.84 low field energy in core radius have been achieved.

For small D, we obtain fundamental-like fields patterns as in Fig. 4.5(a), whereas for larger D we obtain more complicated field patterns that are, however, better confined in the solid core as in Fig. 4.5(c). For a given mode with strong solid-core confinement, we then chose D to maximize the fraction of the electric-field energy (ε |**E**|2) in the core. This is desirable in solid-core fiber applications to reduce absorption loss from the cladding and increase light-gas interactions [1]. The field profile is still strongly confined at a non-zero axial wave vector (β a/2π = 1.99), as shown by the inset.

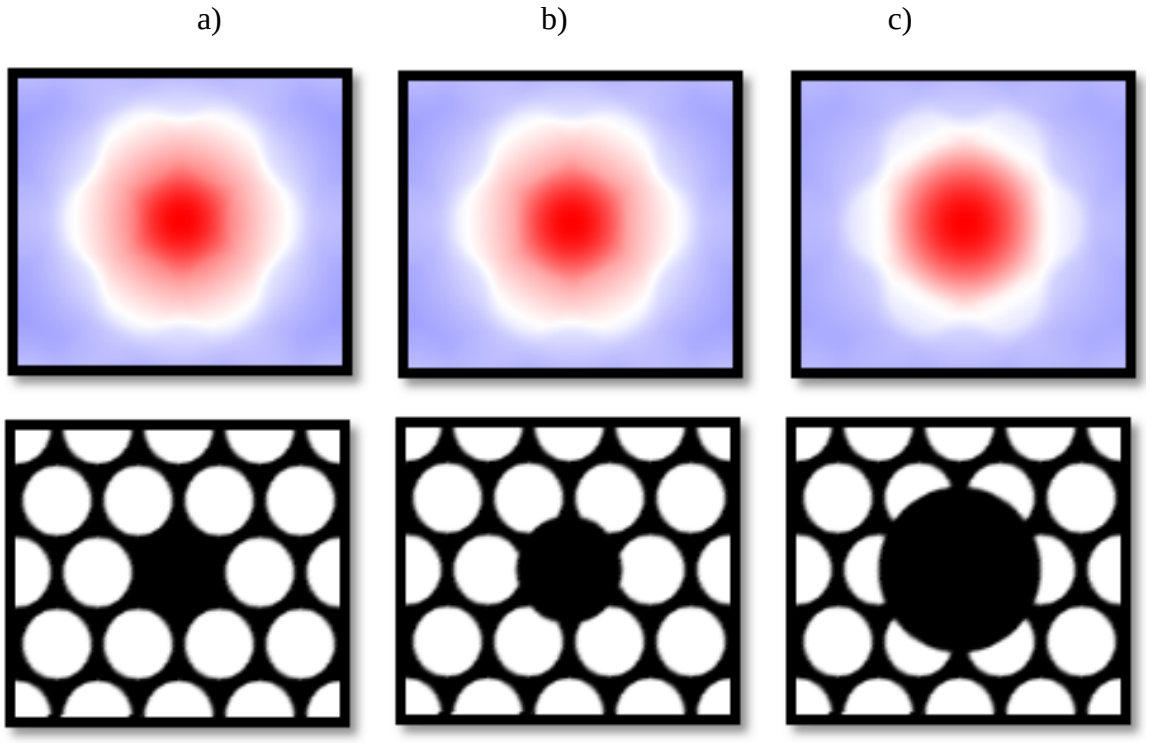

Figure: 4.5 Defect modes for a triangular lattice of cylindrical-shaped holes with periodicity a obtained by varying inscribed defect diameter of a cylindrical-shaped solid core: a) D = 0.50*a*) b) D = 1.40*a* c) D = 2.00*a*

4.2.2 Variation of Fraction of Electromagnetic Energy versus Radius of Core Defect at Different Dielectric Constant:

Fig. 4.6 shows the variations of electromagnetic energy of PCF with the radius of core defect (r) for various values of dielectric constant (ε) at lattice constant (*a*) = 0.9. It can be concluded that electromagnetic energy increases as Radius of core defect (r) increases as a whole. For high values of, radius of core defect periodicity effect doesn't support its function, as fluctuations can be observed for core radius values is 0.1*a* to 0.4*a*.

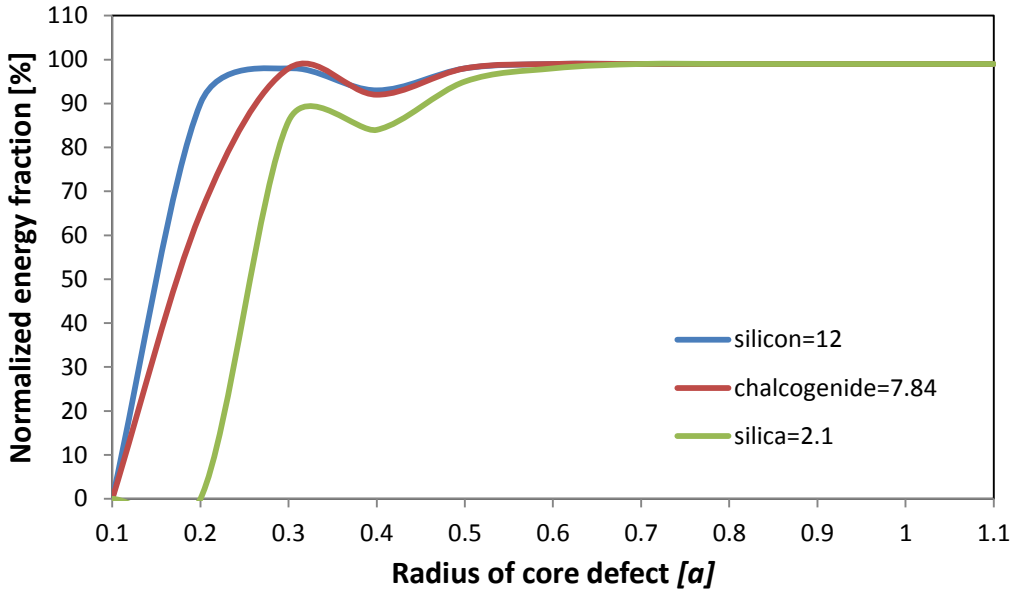

Figure: 4.6 The fraction of electromagnetic field energy localized inside the core-defect. The defect radius is varied between 0.20*a* and 0.90*a*. The size of super-cell is 4 × 4 of the unit cell and holes radius 0.42*a*, *a* = 0.9.

4.3 PCF with Low Group Velocity

Photonic-crystal holey fibers have been of very interest for a variety of different applications, Researchers have also studied photonic-crystal fiber-like geometries with high index contrast materials (e.g. chalcogenide dielectric constant ∼ 7.84) and shown that they support interesting low group-velocity modes but to our knowledge such modes have not been described for fibers made of easily drawable materials. In this work, we demonstrate the possibility of obtaining low group velocity modes in uniform fiber geometries using silicon (constant ∼ 12), which have proven to drawn microstructure fibers. Holey fibers, formed by a lattice of air holes in the fiber cross section, are best known for supporting "finger-like"

band gaps opening towards the high-frequency regime. In the first step, we have designed a PCF as shown in Fig. 4.3. This PCF comprises 4 air hole rings, embedded in pure silicon with a dielectric constant of 12. The radius of the holes in the all inner rings is chosen to be 0.42*a*. The lattice structure of the cladding in this PCF is square and the spacing between the centers of adjacent holes is 1. In solid core PCF, the holes closer to the core have a stronger impact on dispersion. A lower ratio of diameter in the cladding reduces the dispersion and its slope, therefore in this design the holes of the inner rings are chosen to be smaller. On the other hand, increasing the diameter results in reduction of the dispersion, hence the choice of larger diameter for the holes in outer rings. By omitting the holes in the six corners of cladding in the structure, PCF will have even less dispersion.

One 2d photonic crystal structure that is well known to have a complete gap for sufficiently large index contrast is a triangular lattice (period a) of cylindrical air holes (radius r) in dielectric similar to the geometry of many fabricated holey fibers. This geometry with r = 0.42*a* turns out to have a small gap at β = 0 for a dielectric constant of 12. We also considered a slightly modified 2d photonic crystal consisting of a triangular lattice of dielectric rods in air connected by thin veins (resembling cylindrical-shaped holes). The gap in this structure persisted for dielectric contrasts as 12:1. The Maxwell Eigen problem was solved with an iterative (conjugate gradient) method in a plane wave basis. The resulting band diagrams, that extends over a range of nonzero β [1].

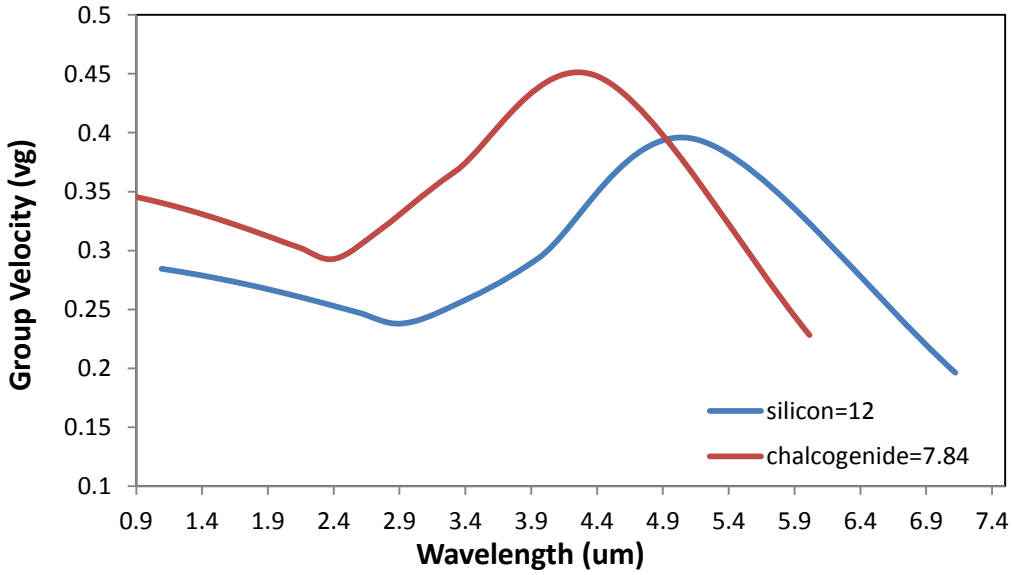

Figure: 4.7 Normalized group velocity obtained by varying the wavelength for different dielectric constant in a photonic crystal fiber.

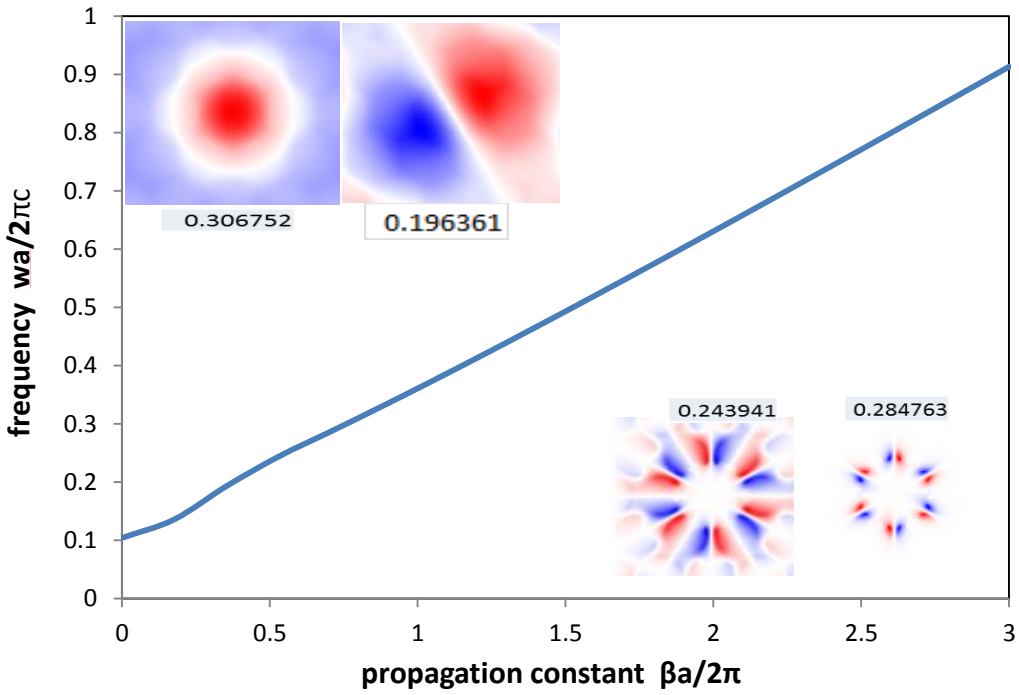

Figure: 4.8 Solid-core guided mode in gap with insets showing electric-field *Ez* and group velocity (vg), (blue/white/red = negative/zero/positive).

One source of loss is the material absorption in the cladding. For a guided mode in the hollow core, this absorption loss is suppressed by a feature of *fc/vgn*, where *f* is the fraction of the electric-field energy in the cladding, *vg* is the group velocity, and *n* is the cladding refractive index. For the mode at β *a*/2π = 0.176, where *vg* = 0.19*c* and *f* =0.03, the absorption loss of the mode is therefore 0.157dB/m, which is sufficient for short-distance fiber devices.

4.4 Variation in Group Index (ng) versus Frequency at Different Material:

Fig.4.10 shows the effective group index versus frequency at various values of dielectric constant on taking photonic crystal fiber parameters, is diameter of air-holes 0.42*a*, N=4×4. It is noticed that on increasing the value of frequency from 0.5 to 0.9, the group index curve attain flatness. At 7.84 of dielectric constant the curve shows great variation in group index in range of frequency 0.1 to 0.4. Whereas it is observed that group index has a flat curve for a dielectric constant of 12.

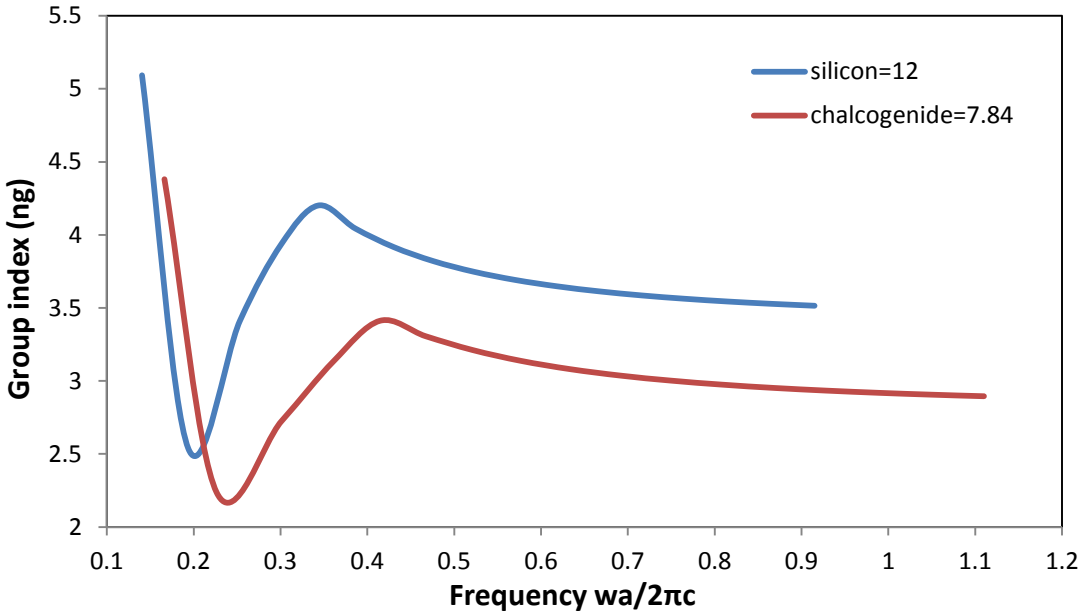

Figure: 4.9 group index *ng* vs. frequency for different values of dielectric constant. Photonic crystal fiber parameter size of the super-cell is 4 × 4 of the unit cell and holes radius 0.42*a*.

4.5 Effect on Dispersion by Various Parameters:

4.5.1 Variation of Dispersion versus Diameter of Air Holes for Different Values of Hole Dielectric Constant:

Fig. 4.11 shows variations in group velocity dispersion with diameter of solid core holes for different values of dielectric constant.

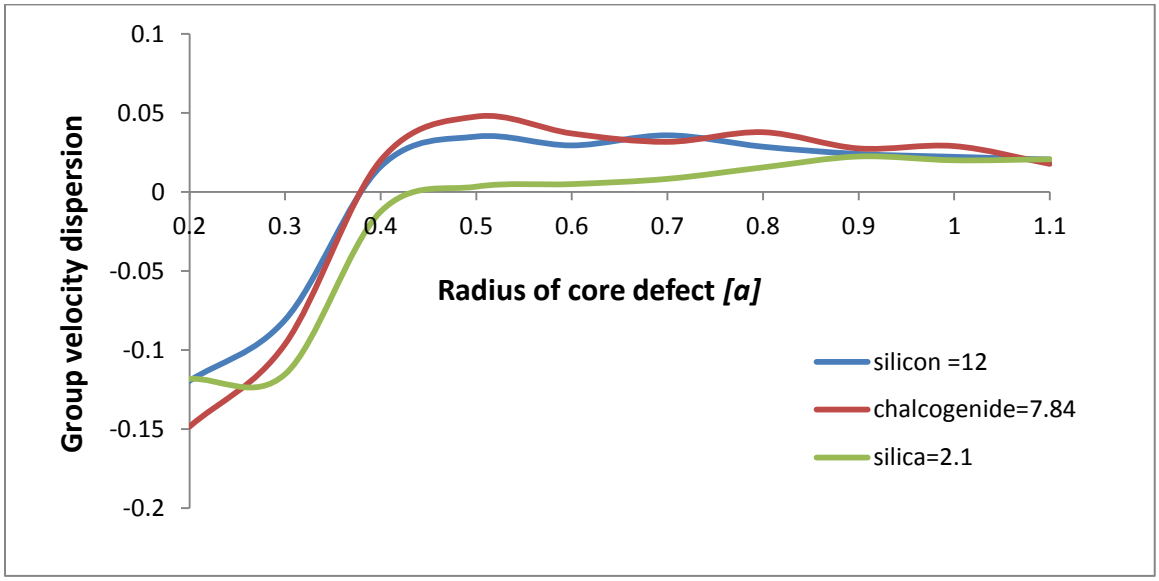

Fig: 4.10 Effect of radius of core defect (r) on the Dispersion at different values of dielectric constant (ε), N=4.

It can be seen that group velocity dispersion becomes near zero and negative initially with increasing hole radius. With further increase in the value of r, it attains a maximum value in positive direction and increases in positive direction afterwards. The optimized value obtained for group velocity dispersion is 0.0358ps/km/nm at r=0.70*a*, dielectric constant=12.

4.5.2 Variation of dispersion versus wavelength (λ) for various values of dielectric constant (ε) of the core:

In addition, different glasses (dielectric constant) can also be exploited, since in this way both Group velocity and group velocity dispersion can be tailored. Fig 4.12 presents a comparison between three PCFs for identical geometric parameters, 4 layers, r=0.42*a* (*a* is lattice constant) but with different materials: (ε=2.1), (ε=7.84) and (ε=12). It can be seen from that negative dispersion increases as wavelength increases for different values of dielectric constant. Although we get largest negative value of dispersion at ε=12 beyond λ=2.6μm point but dispersion is constantly flat at large wavelength for ε=2.1. As we change the dielectric constant (ε) the negative peak is shifted towards the longer wavelength and optical communication is dealing near the λ=1.55μm, hence choice of selecting ε=12 for this thesis was quiet obvious.

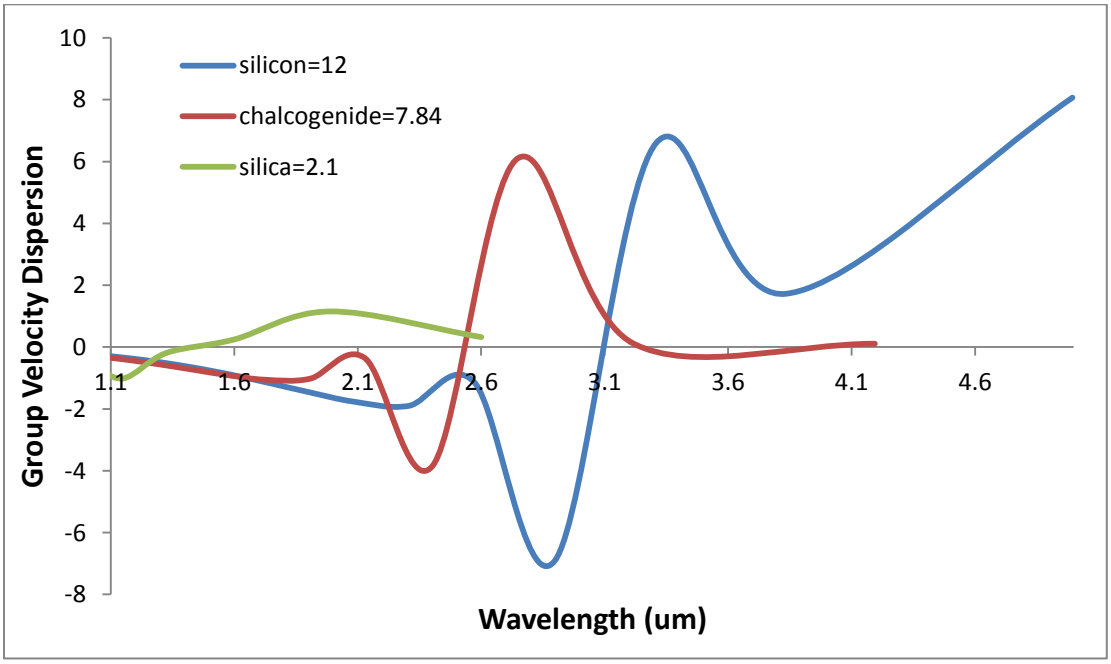

Figure: 4.11 Variation of wavelength (λ) on dispersion at various values of dielectric constant (ε), N=4, r=0.42*a* (*a* is lattice constant).

Profile	Dielectric constant of material (ε)	fraction of electro-magnetic field energy	Group velocity (vg)	Group index (ng)	Group velocity dispersion (ps/nm/km)	Wavelength Range(um)
1.	12 (silicon)	99%	0.19c	5.092	-0.3420 to -1.1324	1.15 to 2.55
2.	7.84 (chalcogenide glasses)	99%	0.22c	4.381	-0.2688 to -0.35366	1.00 to 2.12
3.	2.1 (silica)	98%	0.38c	2.588	-0.9875 to -0.5376	0.59 to 1.00

Table: 4.1 Showing various PCF profiles with Number of layers (n) = 4, hole radius 0.42*a*, core defect radius 0.70*a (a* is Lattice constant).

The optimized PCFs have been designed by taking into account the effects provided by the increase of dielectric constant step and the suitable choice of PCF design parameters (number of air holes rings, hole sizes and inter-hole spacing) and all the calculated profiles have been depicted in Table 1. It has been proposed a four ring PCF with hole radius 0.42*a* and defect core radius 0.70*a* for all the profiles. Profile no.1 provides maximum dispersion in the largest possible wavelength window of 1.15 to 2.25μm, in which the dispersion varies from -0.3420 to -1.1324 ps/nm/km, providing a group velocity 0.19c at ε=12. For profile 2 with ε= 7.84 low ultra-flattened group velocity dispersion in a range -0.2688 to -0.35366 ps/nm/km with group velocity 0.22c has been achieved within the wavelength range of 1.00um to 2.12μm. Largest negative ultra-flattened dispersion ranging from -0.9875 to -0.5376 ps/nm/km has been achieved with profile 3 for which group velocity touching the value of 38c. Thus a tradeoff has been done between low dispersion value and large wavelength range. Hence profile 1 provided the most suitable results with low dispersion & low group velocity with respect to profile 2 and large wavelength window compared to profile 3.

CHAPTER 5

CONCLUSIONS

This thesis targets at the design and simulation of solid-core photonic band gap fibers with large electric field distribution, low group velocity and low group velocity dispersion. A detailed numerical study on the impact of core geometry on the transmission performance of realistic solid-core fibers designs was carried out. Cladding absorption loss values are also calculated to analyze the structure more accurately.

An easy-to-implement design of PCF with small group velocity and a small dispersion slope has been proposed. The dispersion properties of PCF has been tailored with simple structural variations in PCF such as dielectric constant, number of air holes rings, holes sizes and inter-hole spacing and all the calculated profiles have been depicted in Table 1. Four ring PCF with holes radius 0.42*a* and radius of core defect 0.70*a* (*a* is lattice constant) for all the profiles has been proposed. Profile number1 with ε=12, provides maximum electric field distribution and low group velocity dispersion in the largest possible wavelength window of 1.15 to 2.55μm, in which the dispersion varies from -0.3420 to –1.1324 ps/nm/km, providing a group velocity 0.19c. For profile 2 with ε=7.84, flattened group velocity dispersion in a range of -0.2688 to -0.3536 ps/nm/km and group velocity 0.22c have been achieved within the wavelength range of 1.00 to 2.12μm. Largest negative group velocity dispersion ranging from -0.9875 to -0.5376 ps/nm/km has been achieved with profile 3, for which group velocity touched the value of 0.38c within the minimum wavelength window of 0.59 to 1.00μm. Hence profile 1 provided the most suitable results with low dispersion & low group velocity with respect to profile 2 and large wavelength window as compared to profile 3. Cladding loss is made to remain below 0.157dB/m for the proposed design.

The proposed design is easy to implement because of the simplicity of structural variation of PCF and it can be used to compensate dispersion and low group velocity in the long-haul optical fiber links and for gas sensor applications.

REFERENCES

1) Ardavan F. Oskooi, J. D. Joannopoulos, and Steven G. Johnson, **"Zero–group-velocity modes in chalcogenide holey photonic-crystal fibers,"** Vol. 17, No. 12 / **OPTICS EXPRESS** 10083, 2009.

2) D. B. Keck, R. D. Maurer and P. C. Schultz**, "Ultimate lower limit of attenuation in glass optical waveguides,"** Appl. Phys. Lett., vol. 22, pp. 307–309, 1973.

3) P. Kaiser, E. A. J. Marcatili and S. E. Miller, **"A new optical fiber,"** Bell Syst. Tech. J. vol. 52, pp. 265–269, Feb. 1973.

4) P. Yeh and A. Yariv**, "Bragg reflection waveguides,"** Opt. Commun., vol. 19, pp. 427–430, Dec. 1976.

5) P. Yeh, A. Yariv and C.-S. Hong, **"Electromagnetic propagation in periodic stratified media. I. General theory,"** J. Opt. Soc. Am., vol. 67, pp. 423–438, Apr. 1977.

6) P. Yeh, A. Yariv and E. Marom, **"Theory of Bragg fiber,"** J. Opt. Soc. Am., vol. 68, pp. 1196–1201, Sept. 1978.

7) E. Yablonovitch, **"Inhibited spontanous emission in solid-state physics and electronics,"** Phys. Rev. Lett., vol. 58, pp. 2059–2062, May 1987.

8) S. John, **"Strong localization of photons in certain disordered dielectric superlattices,"** Phys. Rev. Lett., vol. 58, pp. 2486–2489, June 1987.

9) J. D. Joannopoulos, J. N. Winn and R. D. Meade**, "Photonic Crystals: Molding the Flow of Light"**. Princeton: Princeton Univ. Press, 1995.

10) J. C. Knight, T. A. Birks, P. S. J. Russell and D. M. Atkin**, "All-silica single-mode optical fiber with photonic crystal cladding,"** Opt. Lett., vol. 21, pp. 1547–1549, Oct. 1996.

11) T. A. Birks, J. C. Knight and P. S. J. Russell, **"Endlessly single-mode photonic crystal fiber,"** Opt. Lett., vol. 22, pp. 961–963, July 1997.

12) J. C. Knight, J. Broeng, T. A. Birks and P. S. J. Russell, **"Photonic band gap guidance in optical fibers,"** Science, vol. 282, pp. 1476–1478, Nov. 1998.

13) R. F. Cregan, B. J. Mangan, J. C. Knight, T. A. Birks, P. S. J. Russell, P. J. Roberts and D. C. Allan**, "Single-mode photonic band gap guidance of light in air,"** Science, vol. 285, pp. 1537–1539, Sept. 1999.

14) J. Broeng, S. E. Barkou, T. Søndergaard and A. Bjarklev, **"Analysis of air-guiding photonic bandgap fibers,"** Opt. Lett., vol. 25, pp. 96–98, Jan. 2000.

15) P. Vukusic and J. R. Sambles, **"Photonic structures in biology,"** Nature (London), vol. 424, pp. 852–855, Aug. 2003.

16) J. Broeng, D. Mogilevstev, S. E. Barkou and A. Bjarklev, **"Photonic crystal fibers: A new class of optical waveguides,"** Optical Fiber Technology, vol. 5, pp. 305–330, 1999.

17) P. Russell, **"Photonic crystal fibers,"** Science, vol. 299, pp. 358–362, Jan. 2003.

18) J. Lægsgaard and A. Bjarklev, **"Microstructured optical fibers– Fundamentals and applications,"** J. Am. Ceram. Soc., vol. 89, pp. 2–12, Jan. 2006.

19) P. J. Roberts, F. Couny, H. Sabert, B. J. Mangan, D. P. Williams, L. Farr, M. W. Mason, A. Tomlinson, T. A. Birks, J. C. Knight and P. S. J. Russell, **"Ultimate low loss of hollow-core photonic crystal fibres,"** Opt. Express, vol. 13, pp. 236–244, Jan. 2005.

20) C. M. Smith, N. Venkataraman, M. T. Gallagher, D. M¨uller, J. A. West, N. F. Borrelli, D. C. Allan, and K. W. Koch**, "Low-loss hollowcore silica/air photonic bandgap fibre,"** Nature (London), vol. 424, pp. 657–659, Aug. 2003.

21) B. J. Mangan, L. Farr, A. Langford, P. J. Roberts, D. P. Williams, F. Couny, M. Lawman, M. Mason, S. Coupland, R. Flea, H. Sabert, T. A. Birks, J. C. Knight and P. S. J. Russell**, "Low loss (1.7 dB/km) hollow core photonic bandgap fiber,"** in Proc. Opt. Fiber Commun. Conf., Los Angeles, CA, 2004.

22) T. D. Engeness, M. Ibanescu, S. G. Johnson, O. Weisberg, M. Skorobogatiy, S. Jacobs and Y. Fink, **"Dispersion tailoring and compensation by modal interactions in omniguide fibers,"** Opt. Express, vol. 11, pp. 1175–1196, May 2003.

23) J. K. Ranka, R. S. Windeler and A. J. Stentz, **"Visible continuum generation in air-silica microstructure optical fibers with anomalous dispersion at 800 nm,"** Opt. Lett., vol. 25, pp. 25–27, Jan. 2000.

24) T. Udem, R. Holzwarth and T. W. H¨ansch, **"Optical frequency metrology,"** Nature (London), vol. 416, pp. 233–237, Mar. 2002.

25) K. Furusawa, A. Malinowski, J. H. V. Price, T. M. Monro, J. K. Sahu, J. Nilsson and D. J. Richardson, **"Cladding pumped Ytterbium-doped fiber laser with holey inner and outer cladding,"** Opt. Express, vol. 9, pp. 714–720, Dec. 2001.

26) J. Limpert, A. Liem, M. Reich, T. Schreiber, S. Nolte, H. Zellmer, A. T¨unnermann, J. Broeng, A. Petersson and C. Jakobsen, **"Lownonlinearity single-transverse-mode ytterbium-doped photonic crystal fiber amplifier,"** Opt. Express, vol. 12, pp. 1313–1319, Apr. 2004.

27) F. Benabid, J. C. Knight, G. Antonopoulos and P. S. J. Russell, **"Stimulated Raman scattering in hydrogen-filled hollow-core photonic crystal fiber,"** Science, vol. 298, pp. 399–402, Oct. 2002.

28) B. J. Eggleton, C. Kerbage, P. S. Westbrook, R. S. Windeler, and A. Hale, **"Microstructured optical fiber devices,"** Opt. Express, vol. 9, pp. 698–713, Dec. 2001.

29) R. T. Bise, R. S. Windeler, K. S. Kranz, C. Kerbage, B. J. Eggleton and D. J. Trevor, **"Tunable photonic band gap fiber,"** in Optical Fiber Communication Conference Technical Digest, 2002.

30) T. T. Larsen, A. Bjarklev, D. S. Hermann and J. Broeng, **"Optical devices based on liquid crystal photonic bandgap fibres,"** Opt. Express, vol. 11, pp. 2589–2596, Oct. 2003.

31) S. G. Johnson and J. D. Joannopoulos, **"Block-iterative frequencydomain methods for Maxwell's equations in a planewave basis,"** Opt. Express, vol. 8, pp. 173–190, Jan. 2001.

32) M.J. Gander, R. McBride, J.D.C. Jones, D. Mogilevtsev, T.A. Birks, J.C. Knight and P.St.J. Russell **"Experimental measurement of group velocity dispersion in photonic crystal fibre"** ELECTRONICS LETTERS Vol. 35 no.1 7th January 1999.

33) R. K. Sinha and Shailendra K. Varshney **"DISPERSION PROPERTIES OF PHOTONIC CRYSTAL FIBERS"** MICROWAVE AND OPTICAL TECHNOLOGY LETTERS / Vol. 37, No. 2, April 20 2003

34) Stig E. Barkon Libori Ph.d thesis **"Photonic Crystal Fiber From Theory to Practice"** feb 28th 2002.

35) Yamiao Wang*, Xia Zhang, Xiaomin Ren, Long Zheng, Xiaolong Liu, Yongqing Huang **"Ultra-flattened chromatic dispersion photonic crystal fiber with high nonlinearity for supercontinuum generation"** Proc. of SPIE-OSA-IEEE/ Vol. 7630 76301F-1

36) B. J. Eggleton, P. S. Westbrook, C. A. White, C. Kerbage, R. S. Windeler and G. L. Burdge, **"Cladding-mode-resonances in air-silica microstructure optical fibers,"** J. Lightwave Technol., vol. 18, pp. 1084– 1100, Aug. 2000.

37) J. C. Knight, J. Arriaga, T. A. Birks, A. Ortigosa-Blanch, W. J. Wadsworth and P. S. Russell, **"Anomalous dispersion in photonic crystal fiber,"** IEEE Photonics Technology Letters, 12(7), 807–809, 2000.

38) A.Ferrando, E. Silvestre, J. J. Miret, and P. Andres, **"Nearly zero ultra flattened dispersion in photonic crystal fibers,"** Optics Letters, 25(11), 790–792, 2000.

39) W. H. Reeves, D. V. Skryabin, F. Biancalana, J. C. Knight, P. S. Russell, F. G. Omenetto, A. Efimov and A. J. Taylor, **"Transformation and control of ultra-short pulses in dispersion engineered photonic crystal fibers,"** Nature, 424(6948), 511–515, 2003.

40) J. C. Knight, J. Broeng, T. A. Birks and P. S. J. Russel, **"Photonic band cap guidance in optical fibers,"** Science, 282(5393), 1476–1478, 1998.

41) J. C. Knight, T. A. Birks, P. S. Russell and D. M. Atkin, **"All-silica single-mode optical fiber with photonic crystal cladding,"** Optics Letters, 21(19), 1547–1549, 1996.

42) T. A. Birks, P. J. Roberts, P. S. J. Russell, D. M. Atkin and T. J. Shepherd, **"Full 2-D photonic bandgaps in silica/air structures,"** Electronics Letters, 31(22), 1941–1943, 1995.

43) R. F. Cregan, B. J. Mangan, J. C. Knight, T. A. Birks, P. S. Russell, P. J. Roberts and D. C. Allan, **"Single-mode photonic band gap guidance of light in air,"** Science, 285(5433), 1537–1539, 1999.

44) J. C. Knight, J. Broeng, T. A. Birks and P. S. J. Russel, **"Photonic band cap guidance in optical fibers,"** Science, 282(5393), 1476–1478, 1998.

45) K Mukasa, M. N. Petrovich, F. Poletti, A. Webb, J. Hayes, A. van Brakel, R. Amezcua- Correa, L. Provost, J.K. Sahu, P. Petropoulos and D.J. Richardson**, "Novel fabrication method of highly-nonlinear silica holey fibers,"** Lasers and Electro-Optics, 2006.

46) Desmond M. Chow*, S. R. Sandoghchi, F. R. Mahamd Adikan **"Fabrication of Photonic Crystal Fibers"** 3rd International Conference on Photonics 2012, Penang, 1-3 October 2012

47) Philip St.J. Russell **"Photonic-Crystal Fibers"** JOURNAL OF LIGHTWAVE TECHNOLOGY, VOL. 24, NO. 12 2006.

48) John D. Joannopoulos, Photonic crystal book**, "modling the flow of light"** second Edition.

49) M.J. Gander, R. McBride, J.D.C. Jones, D. Mogilevtsev, T.A. Birks, J.C. Knight and P.St.J. Russell **"Experimental measurement of group velocity dispersion in photonic crystal fibre,"** ELECTRONICS LETTERS Vol. 35 No. I, 1999.

50) J. D. Joannopoulos, Robert D. Meade and Joshua N. Winn, **"Photonic crystals: molding the flow of light,"** Princeton University Press, Princeton, N.J, 1995.

51) Michela Svaluto Moreolo, Associate Member, IEEE, Gabriella Cincotti, **"Performance Enhancement of Photonic Crystal Slow-Light Devices,"** 978-1-4244-2626-3/08/$25.00,2008

52) R. K. Sinha and Shailendra K. Varshney" **DISPERSION PROPERTIES OF PHOTONIC CRYSTAL FIBERS,"** MICROWAVE AND OPTICAL TECHNOLOGY LETTERS / Vol. 37, No. 2, April 20 2003.

53) Abdelaziz, F. AbdelMalek, S. Haxha, **"Photonic Crystal Fiber With an Ultrahigh Birefringence and Flattened Dispersion by Using Genetic Algorithms"** JOURNAL OF LIGHTWAVE TECHNOLOGY, VOL. 31, NO. 2, JANUARY 15, 2013.

54) Yin Wang, Wei Zhang, Yidong Huang and Jiangde Peng, **"SBS Slow Light in High Nonlinearity Photonic Crystal Fiber,"** Department of Electronic Engineering, Tsinghua University, Beijing, P. R. China 100084.2006

55) Jan Sporik, Miloslav Filka, Vladimír Tejkal, Pavel Reichert, **"Principle of photonic crystal fibers,"** VOL. 2, NO. 2, 2011.

56) J. C. Knight, J. Arriaga, T. A. Birks, Member, IEEE, A. Ortigosa-Blanch, W. J. Wadsworth and P. St. J. Russell, **"Anomalous Dispersion in Photonic Crystal Fiber,"** IEEE PHOTONICS TECHNOLOGY LETTERS, VOL. 12, NO. 7, 2000

57) Alexandre Kudlinski, Rémi Habert, Maxime Droques, Guillaume Beck, Laurent Bigot and Arnaud Mussot **"Temperature Dependence of the Zero Dispersion Wavelength in a Photonic Crystal Fiber"** IEEE PHOTONICS TECHNOLOGY LETTERS, VOL. 24, NO. 6, MARCH 15, 2012.

58) Marzena M. Tefelska, Slawomir Ertman, Tomasz R. Wolinski, Pawel Mergo and Roman Dabrowski **"Large Area Multimode Photonic Band-Gap Propagation in Photonic Liquid-Crystal Fiber"** IEEE PHOTONICS TECHNOLOGY LETTERS, VOL. 24, NO. 8, APRIL 15, 2012.

59) Yani Zhang, Fei Liu, Qiang Xu, Hongyan Gao and Chaojin Wang **"Demonstration of two zero dispersion wavelengths in highly birefringence nonlinear photonic crystal fibers"** The Faculty of Advanced Technology University of Glamorgan Trefforest, Pontypridd, CF37 1RP, UK 2012.

60) Md. Asiful Islam and M. Shah Alam, Senior Member, IEEE **"Design Optimization of Equiangular Spiral Photonic Crystal Fiber for Large Negative Flat Dispersion and High Birefringence"** JOURNAL OF LIGHTWAVE TECHNOLOGY, VOL. 30, NO. 22, 2012.

61) Ran Gao, Yi Jiang, Wenhui Ding and Zhen Wang **"Novel Method for the Measurement of Chromatic Dispersion of Photonic Crystal Fibers"** IEEE PHOTONICS TECHNOLOGY LETTERS, VOL. 25, NO. 2, 2013.

62) Jianhua Li, Rong Wang, Jingyuan Wang, Baofu Zhang, Hua ZhouA novel **"Highly birefringent photonic crystal fiber with hybrid cladding structure"** 2010.

63) S. M. Abdur Razzak, Muhammad Abdul Goffar Khan, Yoshinori Namihira and Md. Yeakub Hussain **"Optimum Design of a Dispersion Managed Photonic Crystal Fiber for Nonlinear Optics Applications in Telecom Systems"** International Conference on Electrical and Computer Engineering ICECE 2008.

64) Tim Birks, Agata Witkowska, Sergio Leon-Saval, Ke Lai, William Wadsworth **"Broadband Mode Convertors in Photonic Crystal Fibres"** on leavefrom the

National Institute of Telecommunications, Szachowa Str. 1, 04-894 Warsaw, Poland 2007.

65) Desmond M. Chow, S. R. Sandoghchi, F. R. Mahamd Adikan **"Fabrication of Photonic Crystal Fibers"** International Conference on Photonics 2012.

66) Assaad Baz, Laurent Bigot, Géraud Bouwmans and Yves Quiquempois, **"Single-Mode, Large Mode Area, Solid-Core Photonic BandGap Fiber With Hetero-Structured Cladding"** JOURNAL OF LIGHTWAVE TECHNOLOGY, VOL. 31, NO. 5, 2013.

67) P. AndrCs, A. Ferrando, E. Silvestre, J.J. Miret and M.V. AndrCs, **"Dispersion and Polarization Properties in Photonic Crystal Fibers,"** 0-7803-7375-8/02/$17.00 2002.

68) Alexandre Kudlinski, Rémi Habert, Maxime Droques, Guillaume Beck, Laurent Bigot and Arnaud Mussot, **"Temperature Dependence of the Zero Dispersion Wavelength in a Photonic Crystal Fiber,"** IEEE PHOTONICS TECHNOLOGY LETTERS, VOL. 24, NO. 6, MARCH 15, 2012.

69) G. Calò, A. D'Orazio, M. De Sario, L. Mescia, V. Petruzzelli, F. Prudenzano, **"Photonic Crystal Fibres"** 0-7803-9236-1/05/$20.00 2005.

70) Saeed Olyaee and Fahimeh Taghipour, **"Ultra-Flattened Dispersion Photonic Crystal Fiber with Low Confinement Loss,"** 11th International Conference on Telecommunications - ConTEL 2011 ISBN: 978-953-184-152-8, June 15-17, 2011.

71) R. Buczynski **"Photonic Crystal Fibers"** information Optics Group, Faculty of Physics, Warsaw University Pasteura 7, 02-093 Warsaw, Poland, No. 2 ,Vol. 106 ,2004.

72) F. BENABID **"Hollow-core photonic bandgap fibre: new light guidance for new science and technology"** Centre for Photonics and Photonic Materials, Department of Physics, University of Bath, Claverton Down, Bath BA2 7AY, UK 2006.

73) **https://www.google.co.in**/search?q=photonic+crystal+fiber&tbm=isch&tbo=u&source=univ&sa=X&ei=u8avU5GREMrIuASM14LwAg&sqi=2&ved=0CDUQsAQ&biw=1366&bi =667

74) H. Kodan and Peter W. Chung **"Simulating Photonic Band Gaps in Crystals"** Computational and Information Sciences Directorate, ARL, june2007.